

Cluster Dynamical Mean Field Theories

G. Biroli,¹ O. Parcollet,¹ and G. Kotliar²

¹*Service de Physique Theorique, CEA Saclay, 91191 Gif-Sur-Yvette, FRANCE*

²*Center for Materials Theory, Department of Physics and Astronomy,
Rutgers University, Piscataway, NJ 08854, USA*

(Dated: November 6, 2018)

Cluster Dynamical Mean Field Theories are analyzed in terms of their semiclassical limit and their causality properties, and a translation invariant formulation of the cellular dynamical mean field theory, *PCDMFT*, is presented. The semiclassical limit of the cluster methods is analyzed by applying them to the Falikov-Kimball model in the limit of infinite Hubbard interaction U where they map to different classical cluster schemes for the Ising model. Furthermore the Cutkosky-t'Hooft-Veltman cutting equations are generalized and derived for non translation invariant systems using the Schwinger-Keldysh formalism. This provides a general setting to discuss causality properties of cluster methods. To illustrate the method, we prove that *PCDMFT* is causal while the nested cluster schemes (NCS) in general and the pair scheme in particular are not. Constraints on further extension of these schemes are discussed.

I. INTRODUCTION

Dynamical Mean Field Theory (for a review see [1]) has been very successful in providing a non perturbative approach to strongly correlated Fermi systems. It describes both the localized and the itinerant limit and has yielded non perturbative insights into the finite temperature Mott transition [1]. This approach has been combined with realistic electronic structure methods such as LDA and GW and has been applied successfully to numerous materials [2]. In spite of these successes, several limitations of the single site *DMFT* approach are now apparent. For example, the self-energy is k independent by construction, so the method cannot describe independent variations of the quasiparticle residue, the quasiparticle lifetime and the effective mass. Furthermore, the single site nature of the method precludes it from treating more exotic orders with order parameters involving several sites, such as dimerization, staggered flux or d -density wave, and d -wave superconductivity.

To overcome these limitations, various extensions of *DMFT* have been proposed. For a disordered system, one can set up a functional integral formulation, with *DMFT* as a saddle point, leading to a natural loop expansion [3]. A formulation of these ideas for a clean system is still lacking. A different extension, is the Extended *DMFT* [4], in which the *DMFT* Ansatz is applied simultaneously to bosonic and fermionic degrees of freedom. This approach does not describe a k -dependent self-energy but incorporate diagrams involving longer range interactions into the *DMFT* equations.

A different idea is based on truncations of the Baym Kadanoff functional. In the full theory, this is a functional of the full Green functions. *DMFT* is obtained by restricting it to local Green functions only, setting the non-local Green functions equal to zero. A natural extension is to restrict the functional to local and nearest neighbor Green functions. This pair scheme was introduced independently by Ingersent and Schiller [5], and by Georges and Kotliar[1]. The latter authors observed non causal behavior in an Iterated Perturbation Theory (IPT) solution of the Hubbard model, but the origin of this problem was not elucidated. Zarand et al. suggested [6] that the pair cluster approach was causal, and that the difficulties encountered in the solution were related to the impurity solver rather than to the scheme itself, but no conclusive proof of this statement was presented. This pair method requires a simultaneous solution of multiple site impurity problems.

A different direction was pursued by Jarrell and collaborators with the introduction of Dynamical Cluster Approximation (*DCA*) [7], whose main idea is to discretize uniformly momentum space. This approach was shown to be manifestly causal. It can also be formulated in real space [8] (See also Appendix A). A different approach, the cellular *DMFT* or *CDMFT*, motivated by applications to electronic structure, was introduced in [9]. In this approach, the many body problem is truncated by introducing a finite basis set of orbitals to truncate the self energy. It introduces the cluster self energy and the lattice self energy as independent entities. This method was tested in a soluble model [8], in the Falikov-Kimball model [10] and in the one dimensional Hubbard model [11]. These papers developed the *CDMFT* ideas from a real space perspective. In this paper we develop this approach from a momentum space perspective, to maintain periodicity in the self consistency equation. The importance of including this periodicity was underlined by Lichtenstein [12, 13] arguing that the lack of periodicity of *CDMFT* could unfavor phases, like the d -wave superconductivity, in which the order parameter lives on links. Even though this point has not yet been elucidated, it is certainly desirable to have a generalization of *CDMFT* that is translation invariant and causal in its use of the lattice self-energy in the self consistency condition.

Cluster *DMFT* methods have not yet reached the level of understanding of their single site counterparts. While the single site *DMFT* can be unambiguously formulated, cluster *DMFT* methods are more diverse and therefore require more detailed methodological investigation, since the virtues and limitations of the various cluster schemes are not apparent yet. This paper is a contribution in this direction.

There are several important principles that a cluster method should satisfy: *i)* Given that cluster *DMFT* approximations are intrinsically basis dependent, a cluster method should be formulated in a general basis set. This flexibility is important, because for a given problem, one could carry out the cluster *DMFT* study in the basis which is most suitable for the system in question. *ii)* It should have an effective action formulation, namely it should target the calculation of a specific correlator function. *iii)* It should yield causal Green functions. *iv)* It should be able to capture the various order, including those which break the translation invariance. *v)* It should converge rapidly as a function of the discretization parameter for the observable that one is targeting. It is possible, that different cluster schemes may converge better for different observables. A better understanding of these elements of a cluster method is desirable.

In section II, we present our translation invariant generalization of *CDMFT* where the lattice self energy participates in the self consistent equation. This is a new cluster scheme, and we formulate it in a way which allows a comparison with *CDMFT* and *DCA*. We also discuss in section II C a different class of schemes, the *nested cluster schemes*, which require the simultaneous consistent solutions of impurity models of different size.

In section III, in an attempt to clarify the nature of the various cluster approximations, we study their classical limit in the Ising limit of the Falikov-Kimball model. The various schemes then reduce to classical cluster approximations to the Ising model. This analysis elucidates their physical content at the classical level and it allows a simple and clear comparison. This study complements other comparisons of cluster schemes against more exact treatments for specific models [8, 10]. The classical limit of *EDMFT* was discussed in [14].

In section IV, we analyze the issue of causality of cluster methods from a diagrammatic perspective using the Cutkovsky-t'Hooft-Veltman rules. We rederive them for non translation invariant cases using the Schwinger-Keldysh formalism. We end up with a general setting to analyze the causality of cluster schemes. Within this framework we show that the pair scheme is not causal, and elucidate the origin of the problem. Furthermore we provide a simple proof of the causality of *CDMFT* and *DCA* (which had already been proved by other methods) and justify the causality of the periodic generalization of *CDMFT*. Finally we make a relationship with the early paper of Mills et al. on disordered systems [15]: in fact the coherent potential approximation (CPA) is a particular case of a *DMFT*. The origin of violations of causality, and their possible cure for the generalizations of CPA were clarified by Mills [15].

II. DESCRIPTION OF THE CLUSTER METHODS

A fairly general model of strongly correlated electrons contains hopping and interaction terms. It is defined on a lattice of \mathcal{N} sites in d dimensions, and we divide the lattice in $(\mathcal{N}/L)^d$ cubic clusters of $S_c = L^d$ sites (more general forms can also be considered). We denote with \mathbf{e}_i the internal cluster position and with \mathbf{R}_n the cluster position in the lattice (therefore the position of the i -th site of the n -th cluster is $\mathbf{R}_n + \mathbf{r}_i$). The lattice Hamiltonian is expressed in terms of fermionic operators $c_{R_n,\alpha}^\dagger$ and $c_{R_m,\beta}$ and can be written as:

$$H = \sum_{n,\alpha,m,\beta} t_{\alpha,\beta}(\mathbf{R}_n - \mathbf{R}_m)c_{R_n,\alpha}^\dagger c_{R_m,\beta} + \sum_{n,\alpha,m,\beta,n',\alpha',m',\beta'} U_{\alpha,\beta,\alpha',\beta'}(\{\mathbf{R}\})c_{R_n,\alpha}^\dagger c_{R_m,\beta} c_{R_{n'},\alpha'}^\dagger c_{R_{m'},\beta'} \quad (1)$$

where $\alpha = i, \sigma$ and σ is an internal degree of freedom (i.e. a spin, spin-orbital or band index). Note that in all this paper, we will denote the position and momentum on the (original) lattice with lowercase letters (r and k) and the position and momentum of the superlattice with uppercase letters (R and K). Different dynamical cluster methods for strongly correlated have been introduced in order to obtain an approximate solution of (1) able to capture the effect of short range (dynamical) correlation and to describe the self-energy k -dependence.

In the following, we introduce a new scheme, the Periodized Cluster Dynamical Field Theory (*PCDMFT*), formulate *CDMFT* and *DCA* in real and k space and the *nested cluster schemes* (*NCS*), i.e. the pair scheme and its generalisations. *CDMFT* [9] is a real-space cluster : the lattice is divided in a superlattice of cells and the scheme is basically the *DMFT* equations on the superlattice [1]. On the other hand, *DCA* [7] is a reciprocal space cluster, where the self-energy in momentum space is approximated by step function around a few points, which we will denote by K_c and are identified to the momentum of the (periodic) cluster. We will show that *PCDMFT* is a natural generalization of both schemes, from a real space and a k -space perspective.

A. Real space perspective

Cluster methods for strongly correlated electrons (*CDMFT*, *DCA*, *PCDMFT*) can be divided in two steps. (Nested cluster schemes will be considered separately).

The first step is the computation of the local cluster propagator $G_{c\sigma\mu\nu}(\tau)$ and the cluster self-energy Σ^C from an effective action containing a Weiss dynamical field $G_{0,\sigma\mu\nu}^{-1}(\tau, \tau')$ and the intra-cluster interaction :

$$S_{\text{eff}} = - \iint_0^\beta d\tau d\tau' c_{\sigma\mu}^\dagger(\tau) G_{0,\sigma\mu\nu}^{-1}(\tau, \tau') c_{\sigma\nu}(\tau') + \int_0^\beta d\tau U_{\alpha\beta\gamma\delta}(R=0) (c_\alpha^\dagger c_\beta c_\gamma^\dagger c_\delta)(\tau) \quad (2a)$$

$$G_{c\sigma\mu\nu}(\tau) = - \langle T c_{\sigma\mu}(\tau) c_{\sigma\nu}^\dagger(0) \rangle_{S_{\text{eff}}} \quad (2b)$$

$$\Sigma^C = G_0^{-1} - G_c^{-1} \quad (2c)$$

where μ, ν are indices for cluster sites. In the following, we will often concentrate on square clusters of linear size L on a d -dimensional square lattice, although many of the results can be generalised easily. Hence, μ, ν will also denote the position of the cluster sites on the lattice : $\mu, \nu \in \mathcal{C} = \{0, \dots, L-1\}^d$ where d is the dimension (intersite distance is normalised to one). We will denote by S_c the cluster's size and by \mathcal{C} the set of cluster points; σ is the spin index as mentioned earlier and $\alpha, \beta, \gamma, \delta$ are double indices gathering the spin and the cluster index.

The second step consists in recomputing the Weiss field using the value of the self-energy obtained by the first step and then iterating until convergence is reached. The real difference between cluster schemes is how the second step is performed.

CDMFT is a direct generalization of *DMFT* to cluster *in real space* and consists simply in rewriting the *DMFT* equations in a matrix form (μ, ν indices are omitted) taking as elementary degrees of freedom all the cluster fermionic degrees of freedom:

$$G_0^{-1}(i\omega_n) = \left(\sum_{K \in \text{R.B.Z.}} \frac{1}{i\omega_n + \mu - \hat{t}(K) - \Sigma^C(i\omega_n)} \right)^{-1} + \Sigma^C(i\omega_n) \quad (3)$$

where $\hat{t}_{\mu\nu}(K)$ is the hopping expressed in the superlattice notations, with K in the Reduced Brillouin Zone (R.B.Z.) of the superlattice. (See Equation A1 in Appendix). Note that from now on the sum over K means always the normalized sum. When convergence is reached and the cluster self-energy has been obtained, the translation invariant lattice self-energy Σ^{latt} ((i, j) denotes a site on the original lattice) is computed by the formula:

$$\Sigma_{i-j}^{\text{latt}}(\omega) = \frac{1}{S_c} \sum_{\substack{\mu, \nu \in \mathcal{C} \\ \mu - \nu = i - j}} \Sigma_{\mu\nu}^C(\omega) \quad (4)$$

Other estimators (that still preserve causality) have been introduced in [8]. Note that in *CDMFT*, the cluster and the lattice self-energy are two different quantities [9] : one has to first solve the cluster problem, and only at the end to compute the lattice self-energy Σ^{latt} . In *CDMFT*, Σ^{latt} does not enter the self-consistency condition.

DCA is more naturally formulated in Fourier space [7]. However it can also be recovered from a real space perspective [8] just changing the hopping matrix in eq. (3) to (See also Appendix A) :

$$\hat{t}_{\mu\nu}^{DCA}(K) \equiv t_{\mu\nu}(K) \exp(-iK \cdot (\mu - \nu))$$

In this case if the self-energy is a cyclic matrix (translation invariant within the cluster) then eq. (3) reduces to (upon diagonalisation) :

$$G_0^{-1}(K_c, i\omega_n) = \left(\sum_{K \in \text{R.B.Z.}} \frac{1}{i\omega_n + \mu - t(K + K_c) - \Sigma^C(K_c, i\omega_n)} \right)^{-1} + \Sigma^C(K_c, i\omega_n) \quad (5)$$

that is the standard *DCA* equation introduced in [7]. Note that if the self-energy is cyclic then the Weiss field computed by (5) will be cyclic, so this property is preserved within the self-consistent loop. In *DCA*, contrary to *CDMFT*, there is no distinction between the cluster and the lattice self-energy. Because it is formulated in k -space, *DCA* is also naturally translation invariant.

We are now ready to define the new scheme, *PCDMFT* for Periodized *CDMFT*. The simplest definition is to take Σ^{latt} in place of Σ^C in the self-consistency condition. This is very close to the scheme proposed by Lichtenstein and

Katsnelson in [13], with the big difference that *PCDMFT* is causal, as will be proved below. Thus the equation relating the self-energy to the Weiss field are:

$$\Sigma_{\text{latt}}(k, i\omega_n) = \frac{1}{S_c} \sum_{\mu, \nu \in \mathcal{C}} \Sigma_{\mu\nu}^{\mathcal{C}}(i\omega_n) \exp(-ik \cdot (\mu - \nu)) \quad (6a)$$

$$G_{\mu\nu} = \sum_k \frac{e^{-ik \cdot \mu} e^{ik \cdot \nu}}{i\omega_n + \mu - t(k) - \Sigma^{\text{latt}}(k, i\omega_n)} \quad (6b)$$

$$G_0^{-1} = G^{-1} + \Sigma^{\mathcal{C}} \quad (6c)$$

where k is in the Brillouin zone of the original lattice.

The three schemes (*CDMFT*, *DCA*, *PCDMFT*) can be summarized into the same matrix equations : Eq. (2) and

$$G_0^{-1}(i\omega_n) = \left(\sum_{K \in R.B.Z.} \left(i\omega_n + \mu - \hat{t}_S(K) - \Sigma_S(K, i\omega_n) \right)^{-1} \right)^{-1} + \Sigma^{\mathcal{C}}(i\omega_n) \quad (7)$$

where the difference between the three schemes is enclosed in the value of t_S and of Σ_S that enter in the self-consistency condition.

Let us now turn to translation invariance breaking phases, where translation invariance is conserved on the superlattice (e.g. antiferromagnet, charge density, “stripes” if the cluster is big enough). *CDMFT* can describe such an order by construction since it does not require the translation invariance. When solved numerically (e.g. with Quantum Monte Carlo method), the translation invariant solutions are often found to be instable towards the ordered one (we have explicitly encountered this phenomenon for example for AF and charge density wave).

DCA and *PCDMFT* require translation invariance, therefore they need to be generalized to handle such an order. For *DCA* there are two solutions for this problem, for example for antiferromagnetic order : *i*) keep a reciprocal space formulation with a Reduced Brillouin Zone and introduce some correlation between k and $k+Q$, with $Q = (\pi, \pi)$ [16]; *ii*) use the *real space formulation* introduced in [8], where translation invariance in the cluster *can* be broken, and look for an antiferromagnetic solution. It is shown in Appendix A that the two approaches are equivalent. However, *i*) *requires to anticipate* the appearance of ordered phase, i.e. to adapt the cluster scheme for the order to be described : one needs to use a special setup for antiferromagnetic order, another for a more complicated order, whereas *ii*) *does not require to anticipate the order* : it will show up automatically solving the real space *DCA* equations with no need to generalize the scheme (provided that the cluster is big enough to contain the unit cell). The same numerical code will produce a translation invariant solution, or an antiferromagnetic one, a stripe-like one. In particular, since translation invariant solution are often found to often be numerically instable, one can not miss a ordered phase with this approach. Therefore, the *real space formulation* of *DCA* is the best solution from a practical point of view.

The *PCDMFT* is unfortunately more complicated to generalize. In the following, we will focus on square clusters on the square lattice. It is useful to introduce a slightly more general formula for Σ^{latt} for a bipartite lattice. The lattice self-energy is a sum of the cluster self-energy put at all possible positions on the lattice. We can rewrite (4) in a more transparent way, as a sum over all possible shifts of the cluster :

$$\Sigma_{\sigma, \mu; \sigma', \nu}^{\text{latt}}(K) = \frac{1}{S_c} \sum_{\delta \in \{0, \dots, L-1\}^d} e^{-iK \cdot (\lfloor \frac{\mu+\delta}{L} \rfloor - \lfloor \frac{\nu+\delta}{L} \rfloor)} L \Sigma_{\sigma, \mu+\delta; \sigma', \nu+\delta}^{\mathcal{C}} \quad (8)$$

where $\lfloor x \rfloor$ is the integer defined by $\lfloor x \rfloor \leq x < \lfloor x \rfloor + 1$ (for a vector it has to be understood component by component), d is the dimension, δ is a d -dimensional shift vector, the bar denotes the modulo reduction by L component by component (adding δ is a circular shift in the cluster).

The idea of the generalization is then simple. In a phase that breaks translation invariance (we take antiferromagnet as an example), we have multiple solutions (two for AF), denoted by an index α ($\alpha = 1, 2$ for AF). In order to respect the order, we need to compensate the shift in the cluster by the change of solution : in the AF example, use one solution on one sublattice, another on the other sublattice. The formula is then

$$\Sigma_{\sigma, \mu; \sigma', \nu}^{\text{latt}}(K) = \frac{1}{S_c} \sum_{\delta \in \{0, \dots, L-1\}^d} e^{-iK \cdot (\lfloor \frac{\mu+\delta}{L} \rfloor - \lfloor \frac{\nu+\delta}{L} \rfloor)} L \Sigma_{\sigma, \mu+\delta; \sigma', \nu+\delta}^{\mathcal{C} \alpha(\delta)} \quad (9a)$$

$$\alpha(\delta) = \begin{cases} 1 & \text{if } \sum_{i=0}^d \delta_i = 0 \text{ [2]} \\ 2 & \text{if } \sum_{i=0}^d \delta_i = 1 \text{ [2]} \end{cases} \quad (9b)$$

For the AF phase and when the original model is $SU(2)$ invariant, the solution $\alpha = 2$ is simply obtain from $\alpha = 1$ by a spin-flip. This does not need to be true in general, either for more complicated order or the Falikov-Kimball

model that we will use in Section III. Let us note however that this generalization is more complex than for the *DCA* scheme from a practical perspective : the expression of Σ^{latt} strongly depends on the order to be described and on the form of the cluster.

B. Reciprocal space perspective. Φ derivation.

We now explore the relation between *PCDMFT*, *CDMFT* and *DCA* from the reciprocal space perspective. In order to do this, we use the generating functional formulation of *DMFT* [1]. Let us recall that one can define a functional $\Gamma(G)$:

$$\Gamma(G) = \text{Tr} \log G - \text{Tr} G_0^{-1} G + \Phi(G) \quad (10)$$

where $G_0 = (i\omega_n - t + \mu)^{-1}$ is the bare propagator and $\Phi(G)$, the Baym-Kadanoff functional, is the sum of all the vacuum two-particle irreducible diagrams constructed with the propagator G and the interaction vertices. The solution of the stationarity equation of (10) is the real propagator of the full interacting theory. *DMFT*, as well as its cluster generalizations, can be seen as an approximation onto $\Phi(G)$. Indeed one obtains the *DMFT* approximation restricting $\Phi(G)$ only to single site propagator (equating to zero all the non single site propagator), i.e. $\Phi_{DMFT}(G) = \sum_i \Phi(G_{ii} | G_{ij} = 0)$ or, equivalently, neglecting the momentum conservation at the vertices. These two procedures, that are equivalent at the single site level, represent two different routes in order to obtain cluster generalization of *DMFT*.

CDMFT can be obtained by a natural real space extension of the *DMFT* approximation on Φ :

$$\Phi_{CDMFT}(G) = \sum_R \Phi(G_{\mu,R;\nu,R} | G_{\rho,R;\lambda,R'} = 0) \quad (11)$$

It's easy to show that the stationarity equation corresponding to this choice of Φ gives back the *CDMFT* equations. Note that the summation of the infinite series of diagram of $\Phi_{CDMFT}(G)$ is performed by the cluster impurity solver like in the *DMFT* case.

DCA is formulated more naturally as an approximation in Fourier space: instead of neglecting completely the momentum vertex conservation one puts a coarse-grained delta inside the complete diagrammatic series.

$$\Phi_{DCA}(G) = N_{ss} \Phi(G(k)) |_{U(k_1,k_2,k_3,k_4)=U_{DCA}(k_1,k_2,k_3,k_4)} \quad (12)$$

where $U_{DCA}(k_1, k_2, k_3, k_4) = \delta_{K_c(k_1)+K_c(k_2), K_c(k_3)+K_c(k_4)} / N_{ss}$, N_{ss} is the number of clusters (number of sites divided by number of sites per cluster) and $K_c(k)$ is a function that for each k gives the center of the $[\frac{\pi}{L}, \frac{\pi}{L}]^d$ cube to which k belongs [7].

PCDMFT has been introduced previously from the real space point of view like a natural generalization of *CDMFT* in which one puts the lattice self-energy inside the self-consistent loop (still preserving the causality properties of *CDMFT*). In the following we shall show that, from the functional point of view, *PCDMFT* can also be seen *at the same time* as a translation invariant formulation of *CDMFT* and as a generalization of *DCA*. Up to now we restricted the discussion to the standard completely localized basis set for simplicity. However, *CDMFT* and *PCDMFT* can be formulated in a general basis set. This flexibility is important, because for a given problem, one could carry out the analysis in the basis which is most suitable for the system in question. As a consequence in the following we will derive *PCDMFT* for a general basis.

We shall show that there are two different procedures leading to the same formulation of *PCDMFT*. Let us focus first on the one which show that *PCDMFT* is the natural translation invariant formulation of *CDMFT*. Call $\varphi_{R\alpha}$ the basis function used to define the cellular *DMFT* [9] and $\tilde{\varphi}_{R\alpha}$ their Fourier transform. Note that they are normalized in such a way that $\sum_i |\varphi_{R\alpha}(i)|^2 = 1$, $\sum_k |\tilde{\varphi}_{R\alpha}(k)|^2 = 1$. The particular case of the standard completely localized basis set corresponds to $\tilde{\varphi}_{R\alpha}(k) = \exp(-ik \cdot x_{R\alpha}) / \sqrt{N}$ (N is the total number of sites). *CDMFT* in a general basis is obtained: *i*) keeping only the intra-cluster interaction: $U_{R_1\alpha, R_2\beta, R_3\gamma, R_4\delta} \rightarrow U_{R\alpha, R\beta, R\gamma, R\delta}$ and *ii*) making the approximation (11) discussed above to the Baym-Kadanoff functional.

PCDMFT can be obtained making the approximations *i*), *ii*) and *imposing* the translational invariance of the original problem. This is performed expressing the propagator in the new basis set in terms of the *translational invariant propagator* in the original basis set:

$$G_{R\alpha, R'\beta}(\omega) = \sum_k \tilde{\varphi}_{R\alpha}(k)^* \hat{G}(k, \omega) \tilde{\varphi}_{R'\beta}(k) \quad (13)$$

Plugging this expression inside the functional leading to *CDMFT* we get the *PCDMFT* functional:

$$\Gamma(\hat{G}(k)) = \text{Tr} \log(\hat{G}) + \text{Tr}((i\omega_n - t(k) + \mu)\hat{G}) + N_{ss} \Phi_{PCDMFT}(\tilde{U}, \hat{G}) \quad (14)$$

where Φ is the Baym Kadanoff functional expressed in terms of $\hat{G}(k)$ and obtained replacing the original matrix of interactions $U(k_1, k_2, k_3, k_4)$ with

$$\tilde{U}(k_1, k_2, k_3, k_4) = \sum_{\alpha, \beta, \gamma, \delta} U_{0\alpha, 0\beta, 0\gamma, 0\delta} \tilde{\varphi}_{0\alpha}(k_1) \tilde{\varphi}_{0\beta}^*(k_2) \tilde{\varphi}_{0\gamma}(k_3) \tilde{\varphi}_{0\delta}^*(k_4) \quad (15)$$

where we made use explicitly of the translation invariance to put $R = 0$.

Extremizing this functional with respect to $\hat{G}(k)$ gives the *PCDMFT* equations together with the form of the lattice self energy:

$$G_{R\alpha, R\beta}(\omega) = \sum_k \tilde{\varphi}_{R\alpha}^*(k) \frac{1}{\omega - \epsilon_k - \Sigma_{latt}(k, \omega)} \tilde{\varphi}_{R\beta}(k) \quad (16a)$$

$$\Sigma_{latt}(k, \omega) = \sum_{\alpha\beta R} \tilde{\varphi}_{R\alpha}^*(k) \Sigma_{\alpha\beta}^c \tilde{\varphi}_{R\beta}(k) \quad (16b)$$

where $\Sigma_{\alpha\beta}^c$ is the self-energy obtained from a cluster impurity problem characterized by a propagator $G_{\alpha, \beta}^c = G_{R\alpha, R\beta}$ and the interaction matrix $\tilde{U}_{\alpha\beta\gamma\delta}$.

As discussed before there is another procedure to get the functional formulation of *PCDMFT* encoded in (14). As the *DMFT* approximation can be obtained just by neglecting the momentum conservation at the vertex, one can interpret (15) as improvement to the *DMFT* approximation in which the vertex is replaced by $\tilde{U}(k_1, k_2, k_3, k_4) = \sum_{\alpha, \beta, \gamma, \delta} \tilde{U}_{\alpha, \beta, \gamma, \delta} \tilde{\varphi}_{0\alpha}(k_1) \tilde{\varphi}_{0\beta}(k_2) \tilde{\varphi}_{0\gamma}(k_3) \tilde{\varphi}_{0\delta}(k_4)$ where $\tilde{U}_{\alpha, \beta, \gamma, \delta} = U_{0\alpha, 0\beta, 0\gamma, 0\delta}$.

At this point a natural question is why we have chosen this particular \tilde{U} and, more interestingly, could other choices lead to a better approximation and what is the procedure to find the “best” \tilde{U} ? Unfortunately we don’t have clear answers to these questions. A partial answer to the first one is that the choice of \tilde{U} leading to *PCDMFT* is the one that we obtain applying the least square minimization to $U(k_1, k_2, k_3, k_4) - \tilde{U}(k_1, k_2, k_3, k_4)$. So in a certain sense it provides the best approximation to U within the chosen basis set. It’s however important to notice that is far from clear that this is a good criterion to select the “best” \tilde{U} . With respect to these remarks is particularly interesting to note that *DCA* can be obtained taking $\tilde{U}_{\alpha, \beta, \gamma, \delta} = U_{0\alpha, 0\alpha, 0\alpha, 0\alpha} \delta_{\alpha, \beta} \delta_{\gamma, \delta} \delta_{\delta, \gamma}$ (in the case of a complete diagonal interaction on the original lattice) and $\tilde{\varphi}_{R\beta}(k) = \exp(-iK_c(k) \cdot x_{R\beta}) / \sqrt{N}$ [7].

This suggests interesting interpolation between *DCA* and *PCDMFT*. A particularly simple one consists in dividing the Brillouin zone in l^d squares (like in *DCA* for a cluster of linear size l) and taking $\tilde{\varphi}_{R\mu}(k) = \exp(-iF_l(k) \cdot x_{R\mu}) / \sqrt{N}$ where $F_l(k)$ is a function such that for each k gives the center of the $[\frac{\pi}{l}, \frac{\pi}{l}]^d$ cube to which k belongs (note that $\mu = 1, \dots, L_c$). When $l = L_c$ one gets *DCA*, whereas when $l = \infty$ one gets *PCDMFT*.

Let us finally note that this functional derivation of *PCDMFT* is crucial to prove simply its causality properties. Indeed this scheme is causal because it is a composition of two causal steps. Clearly starting from a causal cluster self-energy one obtains a causal cluster propagator through (16a, 16b). Furthermore we will show in Section IV that plugging the causal cluster propagator inside the diagrammatic series corresponding to the *PCDMFT* functional gives a causal cluster self-energy.

C. Nested cluster schemes

Another natural generalization of DMFT to the cluster setting is to apply the ideas connected to the *cluster variation method* (CVM) of classical statistical mechanics to the Baym Kadanoff functional [17, 18]. These schemes are also natural generalizations of the n site CPA [19] to interacting electrons. The approach is defined by selecting a set of maximal (namely they are not included in each other) clusters of sites. We denote by Γ the set of maximal clusters together with all its subclusters, and by Φ_α the *restriction* of the Baym Kadanoff functional to $G_\alpha(i, j)$, with $G_\alpha(i, j) = G(i, j)$ if i and j belong to α and $G_\alpha(i, j) = 0$ otherwise. $\tilde{\Phi}_\alpha$ is defined recursively in terms of the Φ_α by $\tilde{\Phi}_\alpha = \sum_{\beta \subset \alpha} \tilde{\Phi}_\beta$ which can be inverted by the Moebius formula $\tilde{\Phi}_\alpha = \sum_{\beta \subset \alpha} (-1)^{n_\beta - n_\alpha} \Phi_\beta$ with n_α the number of sites of cluster α . An approximation scheme is uniquely fixed once a set of maximal clusters is chosen. If the chosen set is invariant under translations, e.g. the set of all plaquettes, we construct a cluster scheme which is manifestly translation invariant by truncating the full Baym Kadanoff functional

$$\Phi \approx \sum_{\alpha \in \Gamma} \tilde{\Phi}_\alpha \quad (17)$$

Differentiation of Φ yields a translational invariant self energy, which requires the solution of several impurity problems. The subclusters of a maximal cluster are generally related among each other by the operations of the crystal group, and fall into different equivalence classes. To compute the lattice self energy one needs to solve several impurity models. One for each representative of inequivalent subclusters of the maximal cluster.

When we take as a set of maximal subclusters the set of all nearest neighbor pairs of the lattice we obtain the pair scheme (or two impurity scheme) [1, 5] which we discuss in more detail for completeness. It is convenient to go back to a lattice notation where lattice sites are denoted by i and j and not by $R\mu$. The approximation to the Φ functional can be written in terms of Φ_1 and Φ_2 which are the Baym Kadanoff functionals of a one and a two impurity problem.

$$\Phi_{pair} = (1 - z) \sum_i \Phi_1[G_{ii}] + \sum_{\langle ij \rangle} \Phi_2[G_{ii}, G_{jj}, G_{ij}] \quad (18)$$

Differentiating this functional gives an equation for the local self energy and the nearest neighbor self energy.

$$\Sigma_{loc} = \frac{\delta\Phi}{\delta G_{ii}} = \frac{\delta\Phi_1}{\delta G_{ii}} + z \left(\frac{\delta\Phi_2}{\delta G_{ii}} - \frac{\delta\Phi_1}{\delta G_{ii}} \right) \quad (19a)$$

$$\Sigma_{nn} = \frac{\delta\Phi_2}{\delta G_{ij}} \quad (19b)$$

The diagrammatic interpretation of the first equation is transparent : each diagram that involves a link is properly counted in the solution of a two impurity model. The diagrams for the local self energy at site i which involve only the Green function at site i , can be obtained from a one impurity model with the correct counting. The contribution of the diagrams for the local self energy which involve the Green functions of a pair of sites, can be obtained by subtracting the contributions from the one and the two impurity self energy and multiplying by z , which results in equation (19a). From Σ_{loc} and Σ_{nn} we can construct the lattice self energy.

$$\Sigma^{latt} = \Sigma_{loc}(i\omega_n) + t(k)\Sigma_{nn}(i\omega_n) \quad (20)$$

and close the equations by requiring the self consistency condition imposed by the Dyson equation [1].

$$G_{loc} = \sum_k \frac{1}{i\omega_n - t(k) - \Sigma_{loc}(i\omega_n) - t(k)\Sigma_{nn}(i\omega_n)} \quad (21a)$$

$$G_{nn} = \sum_k \frac{e^{ik \cdot \vec{\delta}}}{i\omega_n - t(k) - \Sigma_{loc}(i\omega_n) - t(k)\Sigma_{nn}(i\omega_n)} \quad (21b)$$

This can be expressed in the matrix notation, with 2×2 matrices $G = \begin{pmatrix} G_{loc} & G_{nn} \\ G_{nn} & G_{loc} \end{pmatrix}$ and K in the reduced Brillouin zone :

$$G = \sum_{K \in R.B.Z.} (i\omega_n - t(K) - \Sigma^{latt}(K))^{-1} \quad (22)$$

The generalisation of this scheme to antiferromagnetic order is presented in Appendix D. An important feature of this scheme is that the Green function of the one site problem coincide with the diagonal part of the Green function of the two site problem. This is a general ‘‘nested’’ structure for these schemes, hence the name ‘‘nested cluster schemes’’. We will see in section III that this property leads to a quantitatively good classical cluster scheme.

D. Hartree-Fock terms

Another important issue is the treatment of longer range interactions within CDMFT, and PCDMFT. In this context it is worth noticing that the Hartree Fock contribution to the Baym Kadanoff functional (10)

$$\Phi_{HF}[G] = \sum U_{\alpha\beta\gamma\delta}(R_1, R_2, R_3, R_4)(G_{\beta\alpha}(R_2R_1)G_{\delta\gamma}(R_4R_3) - G_{\delta\alpha}(R_4R_1)G_{\beta\gamma}(R_2R_3)) \quad (23)$$

induces a self energy which is frequency independent and therefore does not cause problems with causality and can be evaluated with little computational cost. So it is convenient to separate $\Phi = \Phi_{HF} + \Phi_{dyn}$, and apply the cluster DMFT truncation only to Φ_{dyn} , and to the self energy it generates while treating the Hartree contributions exactly. More precisely, one can treat with Hartree-Fock terms that connect the cluster to the exterior only, to avoid a double counting problem.

This observation is particularly relevant in the treatment of broken symmetries induced by non local interactions as exemplified in the study of the transition to a charge density wave in the extended Hubbard model in one dimension which was studied in ref [11].

III. CLASSICAL LIMIT

In this section, in an attempt to clarify the nature of the various cluster approximations, we investigate analytically the large- U limit of the Falikov-Kimball model, which reduces to the classical Ising model in that case. The Falikov-Kimball model is defined by the Hamiltonian :

$$H = \sum_{\langle i,j \rangle} t_{ij\sigma} c_{i\sigma}^\dagger c_{j\sigma} + U(n_{i\uparrow} - \frac{1}{2})(n_{i\downarrow} - \frac{1}{2}) \quad (24)$$

where $\langle i, j \rangle$ denotes nearest neighbors, $t_{ij\uparrow} = t$ and $t_{ij\downarrow} = 0$. We consider the particle-hole symmetric case ($\mu = 0$). This model has been studied a lot for its own interest (for a review, see [20]), but we will use here as a tool to derive a classical limit for the various cluster methods. This completes the QMC study of this model with CMDFT and DCA [10]. Indeed, in the limit $U \rightarrow \infty$ with $\beta \rightarrow \infty$, $\bar{\beta} = \beta t/U$ fixed, it reduces on the lattice to the Ising model at temperature $1/\bar{\beta}$:

$$H = \sum_{\langle i,j \rangle} J_{i-j}^{\text{Latt}} S_i^z S_j^z \quad (25a)$$

$$J_{i-j}^{\text{Latt}} = t_{ij}/2 \quad (25b)$$

with $S_i^z \equiv (c_{i\uparrow}^\dagger c_{i\uparrow} - c_{i\downarrow}^\dagger c_{i\downarrow})$ (Ising spins). Note that a factor t/U has been absorbed in the definition of $\bar{\beta}$. The proof is analogous to the standard reduction of the Hubbard model to the Heisenberg model : since down electrons are quenched, there is no possible exchange between two spins at different sites, which implies that the interaction is Ising-like. We will now take the classical limit of the various cluster schemes, using their common expression (2) and (7) in order to obtain classical cluster approximations of the Ising model. For the reader not interested in the derivation, we summarize our findings in section III B.

A. Derivation of the classical limit

We first present the derivation of the classical limit of *CDMFT*, *DCA* and *PCDMFT*. Our results on the classical limit of the Pair scheme are presented but derived in appendix D.

In the following, we will concentrate ourselves on square clusters on the square lattice. For clusters with an odd size it is necessary to slightly generalize the *CDMFT* equations to get antiferromagnetism in the usual way, distinguishing two sublattices [1]. To avoid cumbersome notations, we will discuss that point later. The key point is of course that $t_{ij\downarrow} = 0$ makes the model partially solvable in the various schemes.

A priori, we have an effective action given by (2). Since $t_\downarrow = 0$, we can show self-consistently that $G_{0\downarrow}$ is diagonal. Indeed, if $G_{0\downarrow}$ is diagonal, because of the form of the $n_\uparrow n_\downarrow$ vertex, G_\downarrow is diagonal (at all order in U), and so is Σ_\downarrow . In all schemes, $\Sigma_\downarrow^{\text{latt}}$ is then diagonal and independant of K . Therefore from (2), we get for *CDMFT*, *DCA* and *PCDMFT*:

$$(G_{0\downarrow})^{-1}(i\omega_n) = i\omega_n + \Sigma_\downarrow^{\text{C}}(i\omega_n) - \Sigma_\downarrow^{\text{latt}}(i\omega_n) = i\omega_n$$

(For the pair scheme, see Appendix D). Therefore we can consider n_\downarrow as a classical variable and compute the Green function for the up electrons, solving the effective action :

$$S_{\text{eff}} = - \iint_0^\beta d\tau d\tau' c_{\mu\uparrow}^\dagger(\tau) G_{0,\mu\nu}^{-1}(\tau, \tau') c_{\nu\uparrow}(\tau') + \int_0^\beta d\tau c_{\mu\downarrow}^\dagger(\tau) \partial_\tau c_{\mu\downarrow}(\tau) + U \left(n_{\mu\uparrow}(\tau) - \frac{1}{2} \right) \left(n_{\mu\downarrow}(\tau) - \frac{1}{2} \right) \quad (26)$$

where μ, ν are cluster indices. For fixed n_\downarrow , the action for the up electrons is Gaussian, which leads to :

$$G_{\mu\nu} = \sum_{\{n_{\rho\downarrow}=0,1\}} \frac{Z(\{n_{\rho\downarrow}\})}{Z} \left(G_{0\mu\nu}^{-1} - (n_{\mu\downarrow} - \frac{1}{2})U\delta_{\mu\nu} \right)^{-1} \quad (27a)$$

$$Z(\{n_{\rho\downarrow}\}) \equiv \exp \left(\text{Tr} \ln \left(G_{0\mu\nu}^{-1} - (n_{\mu\downarrow} - \frac{1}{2})U\delta_{\mu\nu} \right) \right) e^{\beta U/2 \sum_\rho n_{\rho\downarrow}} \quad (27b)$$

$$Z \equiv \sum_{\{n_{\rho\downarrow}=0,1\}} Z(\{n_{\rho\downarrow}\}) \quad (27c)$$

The computation of the large- U limit is organized in two steps : first, we find the expansion of G_0 , and second we show that in this limit the effective action (27b) becomes the action for a classical Ising cluster with mean-field-like terms. Moreover, the study of the large- U limit requires an expansion in the limit $U \rightarrow \infty$ and $\omega \rightarrow \infty$, with $x = 2\omega_n/U$ fixed. Indeed there is a strong ω dependence at the scale U , as seen already in the atomic limit. We will see that the final result is *not* determined by the $x \rightarrow 0$ limit.

First, we use an Ansatz for G_0 , that we will prove to be consistent

$$G_0^{-1}(i\omega_n) = i\frac{U}{2}x - \Delta(x) \quad (28)$$

with Δ of the order 1 in $1/U$ (plus subdominant terms). Using the expansion

$$(\Lambda - \Delta)^{-1} = \Lambda^{-1} + \Lambda^{-1}\Delta\Lambda^{-1} + \dots$$

with $\Lambda_{\mu\nu} = (S_\mu + ix)\frac{U}{2}\delta_{\mu\nu}$, $S_\mu \equiv 1 - 2n_{\mu\downarrow}$, we expand G_\uparrow in (27a) and obtain from (2c) the following expansion for the cluster self-energy of the up electrons Σ^C :

$$\Sigma_{\mu\nu}^C \equiv \Sigma_{\mu\nu}^{C\text{diag}} + \delta\Sigma_{\mu\nu}^C \quad (29a)$$

$$\Sigma_{\mu\nu}^{C\text{diag}} = -\frac{U\delta_{\mu\nu}}{2} \left(\frac{1}{\langle h_\mu \rangle} - ix \right) + O(1) \quad (29b)$$

$$\delta\Sigma_{\mu\nu}^C \equiv (1 - \delta_{\mu\nu})\Delta_{\mu\nu} \frac{\langle h_\mu h_\nu \rangle_c}{\langle h_\mu \rangle \langle h_\nu \rangle} + O\left(\frac{1}{U}\right) \quad (29c)$$

$$h_\mu \equiv \frac{1}{S_\mu + ix} \quad (29d)$$

where $\Sigma^{C\text{diag}}$ (resp. $\delta\Sigma^C$) is the diagonal (resp. off-diagonal) part of the matrix, the brackets denote the average over $n_{\mu\downarrow}$ or S_μ with the weights defined in (27a). The averages and correlations of h_μ are computed using $S_\mu = \pm 1$ and solving for the probability of the spin to be ± 1 as a function of the correlations:

$$\langle h_\mu \rangle = \frac{\langle S_\mu \rangle - ix}{1 + x^2} \quad (30a)$$

$$\langle h_\mu h_\nu \rangle = \frac{\langle S_\mu S_\nu \rangle - ix(\langle S_\mu \rangle + \langle S_\nu \rangle) - x^2}{(1 + x^2)^2} \quad (30b)$$

For (μ, ν) nearest neighbors in an antiferromagnetic phase, as well as in the paramagnetic phase, we have $\langle S_\mu \rangle + \langle S_\nu \rangle = 0$ and thus:

$$\frac{\langle h_\mu h_\nu \rangle_c}{\langle h_\mu h_\nu \rangle} = \frac{\langle S_\mu S_\nu \rangle_c}{\langle S_\mu S_\nu \rangle - x^2} \quad (31)$$

We now take the limit in the self-consistency condition (7). We keep Σ_S to derive a general formula, and we will specialize to various schemes later. We only use the fact that the diagonal part of Σ_S is independent of K and equal to the cluster self-energy : $\Sigma_{S\mu\mu} = \Sigma_{\mu\mu}^C$. This is true for the schemes studied in this paragraph : *PCDMFT*, *CDMFT* and *DCA* (For the pair scheme, see Appendix D). Therefore, the dominant part of order U in Σ_S is diagonal and we have :

$$\Sigma_S(K) = \Sigma_{\mu\nu}^{C\text{diag}} + \delta\Sigma_S(K) \quad (32)$$

where $\delta\Sigma_S$ is a matrix of order $O(1)$ in the $1/U$ expansion. Denoting with a bar the normalized sum of the reduced Brillouin zone,

$$\overline{A(K)} \equiv \frac{\sum_{K \in \text{R.B.Z}} A(K)}{\sum_{K \in \text{R.B.Z}} 1}$$

we obtain (R is on the superlattice) :

$$\Delta_{\mu\nu}(x) = \tilde{t}_{\mu\nu}(x) + \frac{2t}{U} J_{\rho}^{\mu\nu}(x) \langle h_{\rho} \rangle + O\left(\frac{1}{U^2}\right) \quad (33a)$$

$$\tilde{t}(x) \equiv \overline{t_S} + \overline{\delta\Sigma_S} - \delta\Sigma^C \quad (33b)$$

$$\begin{aligned} J_{\rho}^{\mu\nu}(x) &\equiv \frac{1}{t} \left(\overline{(t_S + \delta\Sigma_S)_{\mu\rho} (t_S + \delta\Sigma_S)_{\rho\nu}} - \overline{(t_S + \delta\Sigma_S)_{\mu\rho}} \overline{(t_S + \delta\Sigma_S)_{\rho\nu}} \right) \\ &= \frac{1}{t} \sum_{R \neq 0} (t_S + \delta\Sigma_S)_{\mu\rho}(R) (t_S + \delta\Sigma_S)_{\rho\nu}(-R) \end{aligned} \quad (33c)$$

Note that \tilde{t} is purely off-diagonal. In the expression of J , $\delta\Sigma_S$ has to be expanded to order $O(1)$ only. Moreover, only the off-diagonal part (in site index) is important since the on site part is restricted to $R = 0$. $\delta\Sigma_S$ and Δ are determined by Eqs. (29, 33) and the relation between Σ_S and Σ^C .

At this stage, it is useful to distinguish two cases depending on the validity of the cancellation

$$\overline{\Sigma_S} \stackrel{?}{=} \Sigma^C \quad (34)$$

In *CDMFT* and *DCA*, $\Sigma_S = \Sigma^C$ is K -independent, therefore (34) holds and $\delta\Sigma_S$ drops out of (33c). \tilde{t} and J do not depend on x , although $\langle h_{\mu} \rangle$ does. In *PCDMFT* however, (34) does not hold and we have to solve for $\delta\Sigma_S$ and Δ (See below) to complete the computation of G_0 .

The second step of the computation is to take the large- U limit of the effective action (26) using the value of G_0 (33). In that limit, we expect that the problem becomes classical, and more precisely for $U \rightarrow \infty$:

$$\langle c_{\sigma\mu}^{\dagger} c_{\sigma\nu} \rangle \rightarrow 0 \quad \text{for } \mu \neq \nu \quad (35a)$$

$$n_{\mu\uparrow} + n_{\mu\downarrow} \rightarrow 1 \quad \forall \mu \quad (35b)$$

Indeed this can be shown explicitly using (27a) and taking the $U \rightarrow \infty$ limit in the Fermi factors, *after* doing the summation over frequencies. However due to the frequency dependent nature of G_0 in *all* cases, we need to use the functional formalism and not the Hamiltonian formalism as in the derivation of the Ising limit on the lattice. This is presented in detail in Appendix B. In the limit $U \rightarrow \infty$ with $\beta \rightarrow \infty$, $\bar{\beta} \equiv \beta t/U$ fixed, the effective action reduces to the classical action for the cluster *at temperature* $1/\bar{\beta}$ and we obtain a *classical cluster scheme* for the Ising model with an interaction J_{Ising} inside the cluster and an additional mean field term J_B :

$$H_{\text{eff}} = \sum_{\langle \mu, \nu \rangle} J_{\text{Ising}}^{\mu\nu} S_{\mu} S_{\nu} + \sum_{(\mu, \nu)} J_B^{\mu\nu} S_{\mu} \langle S_{\nu} \rangle_{H_{\text{eff}}} \quad (36a)$$

$$J_{\text{Ising}}^{\mu\nu} \equiv \int_{-\infty}^{\infty} \frac{dx}{\pi t} \frac{\tilde{t}_{\mu\nu}^2(x)}{(1+x^2)^2} \quad (36b)$$

$$J_B^{\mu\nu} \equiv \int_{-\infty}^{\infty} \frac{dx}{\pi} \frac{J_{\nu}^{\mu\mu}(x)}{(1+x^2)^2} \quad (36c)$$

where (μ, ν) and $\langle \mu, \nu \rangle$ correspond to a general and a nearest neighbors couple of sites respectively. One has to solve a classical Ising cluster, with self-consistent ‘‘boundary’’ condition represented by J_B , which generalize the usual Weiss field. Of course, if \tilde{t} does not depend on x , we find the same result as in the lattice $J_{\text{Ising}}^{\mu\nu} = J_{\mu-\nu}^{\text{Latt}}$ for nearest neighbors.

Let us now specialize our computations to the three schemes presented in Section II and compute the value of J_{Ising} and J_B for *CDMFT*, *DCA* and *PCDMFT* for square clusters of linear size L on a two-dimensional square lattice and for a general hopping t_{δ} where δ is a lattice vector.

- **CDMFT**

In this case, $\Sigma_S(K) = \Sigma^C$ is K independent and $t_S = t$, which leads to $\tilde{t}(x) = t$ and :

$$J_{\text{Ising}}^{\mu\nu} = J_{\mu-\nu}^{\text{Latt}} \quad (37a)$$

$$J_B^{\mu\nu} = (-1)^L \sum_{R \neq 0} J_{\mu-\nu+R}^{\text{Latt}} \quad (37b)$$

The interaction inside the cluster is the same as in the lattice problem and the J_B term is of order $O(1)$ and is confined to the boundary of the cluster. The boundary term couples a spin to the average value of its “ghost” neighbor in the neighboring cells, this average value being computed in the cluster itself using the translation invariance on the superlattice. We added a $-$ sign for odd cluster size, since in this case, the *CDMFT* has to be generalized like *DMFT* with two sublattices in order to capture antiferromagnetism : this is equivalent to reversing the sign of the “ghost” neighbor. In the large cluster limit $L \rightarrow \infty$, the boundary terms play no role and we therefore recover the lattice Ising problem. Notice however that the one dimensional case is pathological since the two boundary terms communicate with each other resulting in a finite T_c in the limit of infinite size. This pathology disappears in higher dimensions and explains the results of reference [10].

• DCA

In $d = 2$, we use a square cluster of linear size $L = 2L_c$, corresponding to L_c K_c points (Cf Appendix A). With the definition $\text{sin}_c(\vec{x}) \equiv \prod_{i=1}^d \sin(x_i)/x_i$:

$$J_{\text{Ising}}^{\mu\nu} = \frac{t}{2} \left(\sum_{\delta=\mu-\nu[2L_c]} \frac{t_\delta}{t} \text{sin}_c \left(\frac{\pi\delta}{2L_c} \right) \right)^2 \quad (38a)$$

$$J_B^{\mu\nu} = \frac{t}{2} \sum_{\substack{\delta, \delta' \\ \delta=\mu-\nu[2L_c] \\ \delta'=\mu-\nu[2L_c]}} \frac{t_\delta t_{-\delta'}}{t^2} \text{sin}_c \left(\frac{\pi(\delta - \delta')}{2L_c} \right) - J_{\text{Ising}}^{\mu\nu} \quad (38b)$$

J_B is the same for all links as required by translation invariance in the cluster. For the first neighbor hopping, denoting by J^{Latt} the value of J_{i-j}^{Latt} for i, j nearest neighbors, the formula reduce to :

$$J_{\text{Ising}}^{\mu\nu} = \frac{16}{\pi^2} J^{\text{Latt}} \quad J_B^{\mu\nu} = \left(2 - \frac{16}{\pi^2} \right) J^{\text{Latt}} \quad \text{for } L_c = 1 \quad (39a)$$

$$J_{\text{Ising}}^{\mu\nu} = \left(\text{sin}_c \frac{\pi}{2L_c} \right)^2 J^{\text{Latt}} \quad J_B^{\mu\nu} = \left(1 - \left(\text{sin}_c \frac{\pi}{2L_c} \right)^2 \right) J^{\text{Latt}} \quad \text{for } L_c > 1 \quad (39b)$$

Note that in the 2×2 cluster, the hopping is doubled since electrons can hop from one site to the neighbor either directly or using the cyclicity condition. In the large cluster limit $L_c \rightarrow \infty$, we recover the lattice problem: $J_{\text{Ising}}^{\mu\nu} \rightarrow J_{\mu-\nu}^{\text{Latt}}$ and $J_B = O(1/L_c^2)$ [10].

• PCDMFT

This case is more complicated since $\Sigma_S = \Sigma^{\text{latt}}$ is now K dependent, hence $\overline{\Sigma_S} \neq \Sigma^C$, except for diagonal elements. Therefore t and J now depend on x . In order to determine them, we have to solve Eqs. (9,29,33). This is done in Appendix C and we obtain :

$$\tilde{t}_{\mu\nu}(x) = t_{\mu\nu} \frac{\langle h_\mu \rangle \langle h_\nu \rangle}{A(x) \langle h_\mu h_\nu \rangle} \quad (40a)$$

$$J_\nu^{\mu\mu}(x) = (-1)^L A^{-2}(x) \sum_{R \neq 0} \frac{t_{\mu-\nu+R}^2}{t} \quad (40b)$$

$$A(x) \equiv 1 - \frac{1}{S_c} \sum_{\substack{\rho \in C \\ \rho+\delta \in C}} \frac{\langle h_\rho h_{\rho+\delta} \rangle_c}{\langle h_\rho h_{\rho+\delta} \rangle} \quad (40c)$$

where δ is one of the basis vectors of the square lattice.

In $d = 1$ for first neighbor hopping, the last term reduces to

$$A(x) = 1 - \frac{1}{L} \sum_{i=1}^{L-1} \frac{\langle h_i h_{i-1} \rangle_c}{\langle h_i h_{i-1} \rangle}$$

The boundary terms are located as in *CDMFT*. In the large cluster limit $L \rightarrow \infty$, in Eq. (40) the boundary terms are subdominant in the denominator and the terms involving the averages of S cancel, restoring the correct J_{Ising} on the lattice. The J_B term cancels since it is restricted to the boundary.

• Pair scheme

The computation of the classical limit of the pair scheme is a little more involved but similar. We show in Appendix D that *if a magnetic solution exists*, it satisfies the equation of the classical variation method : let's take two cluster problems, the first one with one site (denoted with an index (1)) in a field $-zh$, the second one with two sites (denoted with an index (2)), interacting antiferromagnetically with J^{Latt} and in a field $-(z-1)h$, where $z = 4$ is the connectivity :

$$H^{(1)} = zhS^{(1)} \tag{41a}$$

$$H^{(2)} = (z-1)h(S_1^{(2)} - S_2^{(2)}) + J^{\text{Latt}} S_1^{(2)} S_2^{(2)} \tag{41b}$$

where the field h is determined by the “nested consistency condition”

$$\langle S^{(1)} \rangle = \langle S_1^{(2)} \rangle = - \langle S_2^{(2)} \rangle \tag{42}$$

Solving the classical equations, the critical temperature is given by :

$$(z-1) \tanh(\bar{\beta} J^{\text{Latt}}) = 1 \tag{43}$$

which gives $\bar{T}_c / J^{\text{Latt}} \approx 2.88$.

B. Discussion

Let us recapitulate our results. We applied the cluster dynamical mean field theories to the Falikov Kimball model taking $U \rightarrow \infty$ with $\beta \rightarrow \infty$, $\bar{\beta} = \beta t / U$ fixed. In this case the quantum model reduces to the Ising model and the cluster dynamical mean field approximation to classical cluster methods. *CDMFT* corresponds to a simple mean field theory generalized to clusters: each spin on the boundary is subjected to a mean field representing the interaction with the neighboring spins that do not belong to the cluster. The form of the mean field is the standard one: the antiferromagnetic coupling times the magnetization of the spins. Note that in principle the antiferromagnetic coupling is generated via quantum fluctuations and its value is approximation-dependent. In the case of *CDMFT* one gets the same coupling as the one obtained for the lattice.

The classical limit of *DCA* is different mainly for two reasons: *i*) the mean field is not just on the boundary but it acts on all sites and is equal on sites belonging to the same sub-lattice. This is natural in *DCA* because it's an approximation that preserves the translation invariance (or the reduced translation invariance for the AF phase), in the propagator *and* in the Weiss field; *ii*) the form of the mean field is the standard one but the value of the antiferromagnetic coupling in the mean field and for spins inside the cluster are different from the lattice one (and between themselves). Of course in the limit of infinite cluster they reduce to the lattice value.

PCDMFT is similar to *CDMFT* to the extent that the mean field acts only on the boundary. However, as for *DCA*, the value of the antiferromagnetic coupling in the mean field and for spins inside the cluster are different from the lattice one (and between themselves). Finally, the pair scheme reduces to the classical cluster variation method for two sites.

The self-consistent equations corresponding to these classical cluster schemes can be solved analytically for small clusters and using a classical Monte Carlo method to solve the impurity problem for larger size. With the exception of the cluster variational method, the classical limits of these extensions of *DMFT* do not result in drastic improvements in the estimation of T_c for small cluster sizes. The value of T_c predicted by *DMFT* is the standard mean field one: $4J$ (the connectivity of the lattice is four) which is far from the exact value that is $2.27J$. The value obtained using the NCS scheme with two sites, i.e. the pair scheme, lead to a good improvement: $T_c = 2.88J$. Instead the results for *DCA* and *CDMFT* even for larger sizes (4 by 4, 6 by 6 and 8 by 8 clusters) do not improve the estimate of T_c very much. In fact within error bars of 0.1 we get the $T_c^{(4 \times 4)} = 3.2J$, $T_c^{(6 \times 6)} = 3.J$ and $T_c^{(8 \times 8)} = 2.85J$ (within the error

bars the estimate for T_c are the same for the two schemes). Note that the value obtained with a cluster of 16 sites with DCA and $CDMFT$ reaches the estimate obtained with a cluster of two sites using NCS! The results of $PCDMFT$ are clearly worse than the ones of the two previous methods for the numerical value of T_c which is quite larger than what is obtained by $CDMFT$ and DCA . This can be traced to the lack of cancellation of off-diagonal elements in (34) which implies that the cavity field $\Delta(i\omega_n)$ in $PCDMFT$ is not proportional to the square of the hopping matrix element which is an undesirable feature.

IV. CAUSALITY

In this section, we present a general method to prove the causality of cluster approximations and apply it to various schemes, including $PCDMFT$. As mentioned in section II, there are two equivalent presentations for the equations of $DMFT$ and its extensions : a first one using the Weiss function G_0 , and another one using the Luttinger-Ward functional Φ . Let's examine the causality question in both.

- In the formulation with G_0 , one has to prove that: *i*) If G_0 is causal, G_c and Σ are causal : this is a automatic (as long as one uses a causal impurity solver). *ii*) If Σ is causal, G_0 computed from the self consistency condition is causal. This is the difficult part. It was carried out explicitly for $CDMFT$ in [9] and for DCA in [7].
- In the formulation with Φ , one has to prove that: *i*) Given a causal G , $\Sigma_{skel}(G) = \delta\Phi/\delta G$ is causal; *ii*) Given a causal Σ , the self consistency condition produces a causal G . Here *ii*) is obvious, because of the simple form of the bare propagator. *i*) is the difficult part and this section is devoted to a general method to prove it.

To show that the self-energy is causal we have to prove that the retarded self-energy has a negative imaginary part for all ω , *i.e.* $\text{Im}\Sigma_R(x, x', \omega) \equiv (\Sigma_R(x, x', \omega) - \Sigma_R^*(x', x, \omega))/2i$ is negative. We use the Cutkovsky-t'Hooft-Veltman equation (also known in the literature as "cutting equations") which is extremely useful to discuss causality properties in terms of a diagrammatic expansion. It relates the imaginary part of the self-energy to a sum of cut diagrams. A standard derivation can be found in [21] and it is due to t'Hooft and Veltman. However, we present in Appendix E a simpler and self contained derivation, based on the Keldysh method. Contrary to the previous derivation it does not assume translation invariance, which is important to discuss cluster schemes that break translation invariance. Note however, that this method is limited to zero temperature formalism.

This section is organized as follows : in paragraph IV A, we present the Cutkovsky-t'Hooft-Veltman equations and show how it can be used to prove causality; in paragraph IV B, we apply it to various cluster schemes.

A. The Cutkovsky-t'Hooft-Veltman equation

The Cutkovsky-t'Hooft-Veltman equation gives the imaginary part of the retarded self-energy as a sum of cut diagrams. Let us consider the set of all perturbative connected diagrams $\{D\}$ for the self-energy at zero temperature (for a given approximation) and all possible cuts of these diagrams into two connected parts L and R containing respectively the left and the right external point (if they are the same, we drop the diagram). There are n cut propagators going from left to right and $n-1$ from right to left, at frequency ω_i and indices x_i . We denote by MR the mirror of R defined as the left diagram obtained from R by reversing all arrows. (Cf. Fig. 1 for an illustration). To each left diagram, we associate the value d_L of corresponding $T=0$ diagram, using the $T=0$ Feynman propagator (G^{++} in Keldysh notation : see appendix E). Note that for each given half left diagram one has to put in d_L all the half left diagrams obtained permuting the cut lines in all the possible ways and then multiply by an appropriate symmetry factor discussed in the appendix (E). We then write $D_L(x, \omega, \{x_i\}, \{\omega_i\}) \equiv d_L\theta(\omega) + d_L^*\theta(-\omega)$, where θ is the Heaviside function. We denote all cut propagators with an index i . To each we associate $\rho(x_i, x'_i, \omega_i)\theta(\epsilon_i\omega_i)$ with $\epsilon_i = \text{sgn}\omega$ for a propagator going to the right, $-\text{sgn}\omega$ for a propagator going to the left. The summation over diagrams can be expressed as a summation over n and a sum over diagrams $D_n = (L_n, R_n)$ with a given number of cut propagators going to the right. The Cutkovsky-t'Hooft-Veltman equation is then:

$$\text{Im}\Sigma_R(x, x', \omega) = - \sum_{n \geq 2} \frac{1}{2n!} \sum_{D_n=(L_n, R_n)} \sum_{\substack{\{x_i\} \\ \{x'_i\}}} \int d\omega_i D_{L_n}(x, \omega, \{x_i\}, \{\omega_i\}) (D_{MR_n}(x', \omega, \{x'_i\}, \{\omega_i\}))^* \times \prod_{i=1}^{n_L+n_R} \rho(x_i, x'_i, \omega_i)\theta(\epsilon_i\omega_i) \quad (44)$$

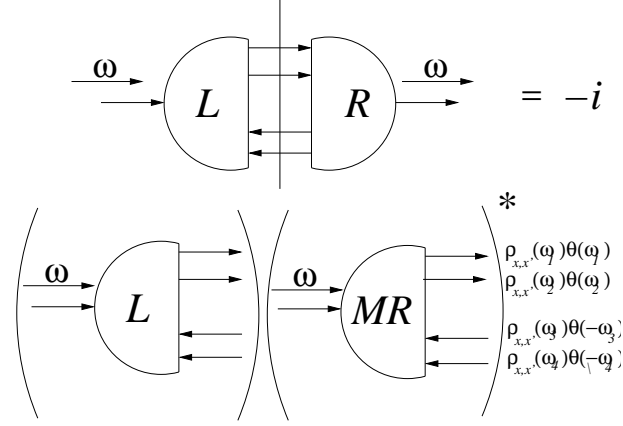


FIG. 1: Definition of cut diagrams

Remark: if the system is translation invariant then we can Fourier transform also with respect to space and get:

$$\text{Im}\Sigma_R(k, \omega) = - \sum_{n \geq 2} \frac{1}{2n!} \sum_{D_n=(L_n, R_n)} \sum_{\substack{\{x_i\} \\ \{x'_i\}}} \int d\omega_i D_{L_n}(k, \omega, \{k_i\}, \{\omega_i\}) (D_{MR_n}(k, \omega, \{k_i\}, \{\omega_i\}))^* \prod_{i=1}^{n_L+n_R} \rho(k_i, \omega_i) \theta(\epsilon_i \omega_i) \quad (45)$$

Note that there are no terms with $n \leq 2$, otherwise the original closed diagram would not be 2PI.

Let us now see how to use (44) to prove causality of the self-energy. We want to show that:

$$\mathcal{A} = \frac{1}{2i} \sum_{x, x'} w_x (\Sigma_R(x, x', \omega) - \Sigma_R^*(x', x, \omega)) w_{x'}^* \leq 0 \quad \forall \{w_x\} \quad (46)$$

for all complex vector w_x . Using eq. (44) we find that we can write the previous quantity as a sum over cut diagrams:

$$\mathcal{A} = - \sum_{\substack{n_L \geq 0 \\ n_R \geq 0}} \frac{1}{2n!} \sum_{D_n=(L_n, R_n)} \sum_{\substack{\{x_i\} \\ \{x'_i\}}} \int d\omega_i \left(\sum_x w_x D_{L_n}(x, \omega, \{x_i\}, \{\omega_i\}) \right) \left(\sum_{x'} w_{x'}^* D_{MR_n}^*(x', \omega, \{x'_i\}, \{\omega_i\}) \right) \times \prod_{i=1}^{n_L+n_R} \rho(x_i, x'_i, \omega_i) \theta(\epsilon_i \omega_i) \quad (47)$$

At this stage, we can use the causality of G , *i.e.* the positivity of $\rho(x, x')$. It implies the positivity of the tensor product $\prod_{i=1}^{n_L+n_R} \rho(x_i, x'_i, \omega_i)$ considered as a matrix of indices $(x_1, \dots, x_{n_L+n_R})$. Hence, positivity of $-\text{Im}\Sigma$ would result if the summation over diagrams could be recast as a square. More precisely, a simple property that implies causality is that for any n :

$$\{(L_n, R_n)\} = \{L_n\} \times \{R_n\} \quad (48)$$

$\{L_n\}$ (resp. $\{R_n\}$) is the set of left (resp. right) parts of diagrams with fixed n . Eq. (48) says that all diagrams can be obtained once and only once using a left part and a right part, which is equivalent to two properties:

- Closure property : With any left part and any right part (that have the same n), gluing them constructs a diagram present in the expansion.
- Exact counting property : all diagram are obtained that way (by definition of left/right parts) but only once : there is no overcounting problem

If the property (48) holds, then using the notation

$$y_n(\{x_i\}; \{\omega_i\}, \omega) \equiv \sum_{x, L_n} w_x D_{L_n}(x, \omega, \{x_i\}, \{\omega_i\})$$

we have :

$$\mathcal{A} = - \int d\omega_i \sum_{n \geq 2} \sum_{\{x_i\}, \{x'_i\}} y_n(\{x_i\}; \{\omega_i\}, \omega) y_n^*(\{x'_i\}; \{\omega_i\}, \omega) \prod_{i=1}^{n_L+n_R} \rho(x_i, x'_i, \omega_i) \theta(\epsilon_i \omega_i) \quad (49)$$

Note that the sum over $\{x_i\}, \{x'_i\}$ inside the integral can be interpreted as the product of the two vectors y and y^* with a positive definite matrix. Thus the positivity of ρ implies the negativity of $\text{Im}\Sigma$.

The efficiency of this method is that one can prove causality, *just by examining the combinatoric structure of the diagrams present in the approximation*, with no further computation. A few remarks are important at this stage : *i)* This method can prove the causality of a scheme, but it can not prove that a scheme will violate causality. In particular it proves the positivity of $-\text{Im}\Sigma$ for all causal propagators G . In the following, we will refer to this as the strong causality property. It is a logical possibility that this property does not hold, while the *actual solution of the scheme* G is indeed causal for all parameters. However, we know no example of this, and the strong property is interesting since we use iterative algorithm to solve the self-consistent impurity problem. *ii)* Equation (48) is sufficient but not necessary : one could also have form squares in a more complicated manner. *iii)* As a remark, we see that the full perturbation theory on the lattice satisfies the property (48) : the full diagrammatic expansion obviously leads to a causal self-energy.

B. Applications

1. CDMFT and DCA

CDMFT can be obtained from the Baym-Kadanoff functional taking $\Phi = \sum_{\mathbf{R}} \Phi(G_{\alpha,\beta}; \mathbf{R}, \mathbf{R})$, where R is the cluster index and α is the internal cluster index. As a consequence $\Sigma_{\alpha,\beta; \mathbf{R}, \mathbf{R}} = \Sigma_{\alpha,\beta} = \frac{\delta \Phi}{\delta G_{\alpha,\beta}}$. Since $\Phi(G_{\alpha,\beta})$ is the sum of all the 2PI diagrams of a L^d lattice, *CDMFT* does satisfy (48) and therefore is a causal scheme.

In *DCA*, one writes the self energy in terms of the complete series of diagrams and the delta function at the vertices are replaced by a coarse grained function. As discussed previously *DCA* is equivalent to replace the Kronecker delta $\delta_{k_1+k_2, k_3+k_4}$ with a Kronecker delta $\delta_{k_1^c+k_2^c, k_3^c+k_4^c}$ where k_i^c is the cluster momentum related to the hypercube containing k_i . Formally $k_i^c = k_i \bmod (\pi/L, \dots, \pi/L)$. Hence, *DCA* satisfies (48) : the proof is the same that for the complete series of diagrams for the self energy. The fact that the k structure of the vertices is different does not change nothing at all. Hence, we see that *DCA* is automatically causal.

2. PCDMFT

The causality of *PCDMFT* is easily established using its real space formulation (9). The causality for *CDMFT* implies the causality of Σ^C . We just have to show that Σ^{latt} is causal. For any complex vector $x_{\sigma\mu}$, we have from (9)

$$\sum_{\sigma\sigma'\mu\nu} x_{\sigma\mu}^* x_{\sigma'\nu} \Sigma_{\sigma,\mu;\sigma',\nu}^{\text{latt}}(K) = \frac{1}{S_c} \sum_{\delta \in \{0, \dots, L-1\}^d} \sum_{\sigma\sigma'\bar{\mu}\bar{\nu}} z_{\sigma;\bar{\mu}}^*(\delta) z_{\sigma';\bar{\nu}}(\delta) \Sigma_{\sigma,\bar{\mu};\sigma'\bar{\nu}}^{C\alpha(\delta)} \quad (50a)$$

$$z_{\sigma;\bar{\mu}+\delta}(\delta) \equiv x_{\sigma\bar{\mu}} e^{iK \cdot \lfloor \frac{\mu+\delta}{L} \rfloor L} \quad (50b)$$

The negativity of Σ^C implies that we have a sum of negative terms. This shows that causality of *PCDMFT* is guaranteed *term by term in the δ sum*.

Note that another way to reach the same conclusion is based on the fact that *PCDMFT* can be interpreted as the solution of a real lattice systems replacing the real $U(k_1, k_2, k_3, k_4)$ with its *PCDMFT* counterpart. Thus, the statement of causality of *PCDMFT* is a particular case of the causality of the original problem with a general U .

3. Non-Causality of the pair scheme

The pair scheme, described in Section II C, has been originally introduced in [1, 5]. It seems a very natural way to introduce systematically a k -dependence for the self-energy. Unfortunately, as we will show in the following, this scheme is not causal for two reasons that we shall discuss in detail.

First, let's apply the Cutkovsky rule. We see that the pair scheme does not satisfy the property (48) or more precisely the closure property. Indeed, when cutting a diagram for Σ , we only have two sites indices i and j . Let consider a cut diagram $(L1, R1)$ where we have i along the cut, and the similar diagram $(L2, R2)$ where j is replaced by $k \neq i, j$. A priori, we could glue the parts into $(L1, R2)$, but that diagram would involve i, j and k , and thus is not present in the diagrammatic expansion generated by the pair scheme. This is a first reason for lack of causality. We stress that this is not a proof, but a quick and strong indication that the scheme is not strongly causal. It's interesting to point out that this problem was already encountered in the case of disordered electron systems when people tried to generalize CPA to clusters. In that case Mills and collaborators [15] noticed that a generalization of CPA similar to the pair scheme has this type of non-closure problem. For this reason they introduced the traveling cluster method which is fully causal. We will comment afterward on the possibility to do the same for strongly correlated electrons.

Let us now really show that the pair scheme is not causal. In fact the violation of the closure property is just an hint that there could be some problem with causality but it doesn't preclude the possibility that eventually the scheme is causal. In the following we will consider the solution of the pair scheme when $U \rightarrow 0$ for an arbitrary bare spectral density or hopping on the original lattice. We will show that a particular choice of the bare spectral density gives rise to a non causal self-energy thus proving in an explicit example the non causality of the scheme.

To study the sign of the imaginary part of the self-energy in the limit $U \rightarrow 0$ one can focus just on the second order term because the first order gives no contribution. Moreover one can replace in the diagram the full propagator with the bare or lattice one ($G_{bare} = (i\omega_n - t - \mu)^{-1}$), the error leading to a term of an order larger than $O(U^2)$. If one applies the Cutkovsky equations to obtain the imaginary part of the self-energy for the second order diagrams of the pair scheme then one has to restrict the sum in the first line of Fig. 2 to single sites (x, x) and links $\langle x, x' \rangle$. The sum over the single sites (x, x) is just the same that one obtains for usual *DMFT* and is clearly positive. The link term $\langle x, x' \rangle$ with x, x' nearest neighbors equals (ω is the (positive) self-energy frequency):

$$U^2 \int_0^{+\infty} d\omega_1 \int_{-\infty}^0 d\omega_2 \sum_{\langle x, x' \rangle} (w_x w_{x'}^* \rho(x, x', \omega_1) \rho(x, x', \omega_2) \rho(x, x', \omega - \omega_2 - \omega_3) + w_{x'} w_x^* \rho(x', x, \omega_1) \rho(x', x, \omega_2) \rho(x', x, \omega - \omega_2 - \omega_3)) \quad (51)$$

The spectral density in the previous equations is just the bare spectral density obtained by t_{ij} . For the pair scheme one can find a spectral density matrix that, injected into the previous equations, does not lead to a causal self-energy. The causality of the spectral density matrix is equivalent to the positivity of each Fourier element $\rho_k(\omega) \geq 0$. However, even if $\rho_k(\omega) \geq 0$, $\rho_{x, x'}(\omega)$ with x, x' nearest neighbors can be negative and as close as possible (in absolute value) to $\rho_{x, x}(\omega)$ for any ω . Consider for example the example in which $\rho_k(\omega)$ is strongly peaked and has an important weight only near the points $\pm\pi, \dots, \pm\pi$. In this case $\rho_{x, x}(\omega) > 0$, $\rho_{x, x'}(\omega)$ with x, x' nearest neighbors is negative and $\rho_{x, x'}(\omega) = \int_{BZ} \frac{dk}{(2\pi)^d} \rho_k(\omega) \exp(-ik(x - x')) \simeq - \int_{BZ} \frac{dk}{(2\pi)^d} \rho_k(\omega) = -\rho_{x, x}(\omega)$. In this case the contribution of (51), for example for $w_x = 1$, is negative and approximatively two times larger in absolute value than the contribution from the x, x term. Since for each x, x term there are z (z is the connectivity) terms like (51) the global sum is negative for $z > 2$, i.e. in any dimension large than one (if one takes a square or cubic or hypercubic lattice). Thus in this case, the self-energy is not causal. So we have found a second reason for non-causality: even if the closure property is verified and in the cutting-folding procedure no new diagrams are created (which is the case for the pair scheme at second order in U) this does not guaranteed that there is a way to write all the cut diagrams as a sum of squares. One can have an overcounting problem as we have just shown for the pair scheme.

Let us now comment on the possibility to cure the pair scheme as Mills and collaborators did in the case of disordered electrons defining the traveling cluster scheme. What they did is to solve the violation of the closure property allowing an arbitrary self energy diagram to have only single site and nearest neighbor propagators. So in this case a self-energy diagram can connect two arbitrary points but just through a sequence of nearest neighbor propagators (that is why the scheme is called "traveling"). This clearly solve the first problem: the non-closure but in principle it doesn't guarantee that the second one also is cured. And indeed it is not for strongly correlated electrons. A simple way to see it is that even with a generalization of this type in the limit $U \rightarrow 0$ the causality counter-example exhibited for the pair scheme is still valid. Instead the case of disordered electrons has a simpler diagrammatics (there are no loops in the self-energy diagrams due to the use of the replica method) and one can explicitly rewrite everything as a sum of squares. In particular the diagram discussed before is simply not there.

A way to circumvent these two difficulties is write the self-energy as the sum of all diagram and then replace the original propagator with a simplified restricted version that is guaranteed to be causal. For example in order to have a causal generalization of the pair scheme, close in spirit to the traveling cluster, one can write:

$$\Sigma = \left. \frac{\delta\Phi}{\delta G} \right|_{G=\tilde{G}} \quad \tilde{G}(k, \omega) = G_0(\omega) + G_1(\omega) \sum_{i=1}^d (2 \cos(k_i))$$

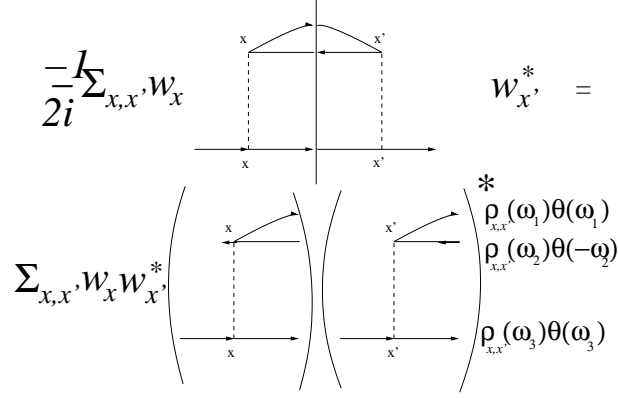


FIG. 2: Example of cut diagram. MR means mirror image of R.

where G_0, G_1 are fixed imposing the conditions $\tilde{G}(0, \dots, 0, \omega) = G(0, \dots, 0, \omega)$ and $\tilde{G}(\pi, \dots, \pi, \omega) = G(\pi, \dots, \pi, \omega)$, and $G = (G_0^{-1} - \Sigma)^{-1}$. This guarantees that \tilde{G} is a causal propagator as long as G is causal. So when \tilde{G} is inserted in the complete series it will give rise to a causal self-energy. The problems with this scheme is that: (1) it seems that it is not Φ -derivable. The reason is that in all the diagrams there are only nearest-neighbor propagator. However since the diagrams connect in general two sites that are not nearest neighbor it is difficult to think how one can obtain it using a restricted set of diagrams for Φ . Note however that is also the case of the traveling cluster scheme for disordered electrons. (2) It is not clear what type of impurity solver, if any, can be used to sum the series of diagrams. In the case of the traveling cluster many simplifications arise that allow one to solve (2) but not (1). the smaller becomes the causality violation. Let us finally remark that the two mechanisms behind the non causality of the pair scheme apply also to the general NCS schemes even though we expect smaller violations of causality for larger clusters.

V. CONCLUSION

Cluster schemes are a promising method for studying strongly correlated electrons. Compared to the study of small finite size systems, they offer the advantage that the thermodynamical limit is taken from the outset, and hence one can hope for smaller finite size effects. As a prime example, we now know that even a one site cluster captures many non trivial features of the Mott transition.

On the other hand, there is no unique generalization of the single site dynamical mean field approximation. Some generalizations view the *DMFT* and its resulting impurity (or multiple impurity models in the case of the NCS) as a trick for summing selected classes of diagrams. An alternative view is provided by the cavity construction and by functional methods, where an effective action is constructed to compute the correlation functions of selected coarsened or cluster degrees of freedom. Finally, one can view *DMFT* as a choice of boundary conditions for finite size studies of a small set of degrees of freedom, where the boundary conditions recognizes that those degrees of freedom are periodically repeated in a medium. While all those points of view, lead to the same set of *DMFT* equations in the single site case, they lead to different constructions for cluster extensions, and the strenghts and limitations of these extensions need to be explored. This paper contributed in this direction by clarifying two important aspects of these extensions, namely the conditions on the cluster scheme needed for the scheme to satisfy causality, and the reduction of the cluster schemes to spin cluster methods in the classical limit.

First, we introduced *PCDMFT* which is a causal generalization of the scheme proposed by Lichtenstein and Katnelson [13]. Second, we provided a general way to prove causality of cluster scheme and showed that the pair scheme, which is the most natural extension in the sense that it is defined by a translational invariant restriction of the Baym Kadanoff functional, is not causal : the diagrammatic reason for the failure of this method was clarified. Third, we also showed formally, in the context of the Falikov Kimball model how the semiclassical limit of the different cluster methods reduce to classical spin cluster methods. Both *DCA* and *CDMFT* give comparable answers even though their Weiss fields have a very different form (in *DCA* the Weiss field is uniformly distributed inside the cluster while in *CDMFT* it is focused on the boundary). On the other hand *PCDMFT*, have an unphysical feature in the classical limit which results from a Weiss field which does not vanish as the square of the hopping matrix elements. The nested cluster schemes are clearly superior and provide a quantum generalization of the cluster variation method which gives

critical temperatures that converge rapidly with cluster size. We showed that the nested cluster schemes violates causality. Our proof suggests that this violation is going to be more severe, when a substantial part of the lattice self energy has a range that exceeds the size of the maximal cluster used in the NCS. On the contrary when the range of the self energy is contained in the maximal cluster, the diagrams generated by the Cutkovsky procedure which are not contained in the NCS are small, which is consistent with the early numerical studies which indicated no violation of causality in the pair scheme at high temperature. This observation is in the same spirit as a recent study of a new (non-nested) scheme, the “fictive impurity model method” , which connected violation of causality with peaks in momentum space in the lattice self energy [22].

An important lesson that can be learned from our results is that the choice of an optimal cluster scheme may depend of the property studied and the physical system at hand. Indeed our semiclassical analysis revealed *PCDMFT* is not accurate in insulating regimes, at least in the one that we focused on doing the semiclassical limit. Instead *CDMFT* performs rather well. We conjecture that *CDMFT* is accurate in insulating cases and *PCDMFT* in metallic cases. Indeed a recent numerical in one dimension work points in this direction ([23]).

Another important result concerns the remarkable accuracy of the NCS scheme compared to the other ones. Even if its performance in a case with stronger quantum fluctuations remains an open question, we think that it would be particularly interesting to try to cure the causality problem keeping the nesting idea inherent to the NCS scheme. Another route to follow is try to incorporate the cellular dynamical mean field ideas of defining impurity models in adaptive basis sets into a NCS scheme. In this way one could try to adapt the basis to the problem so that the resulting self energy is short range and the causality problem, even if not avoided, is sensibly reduced.

Finally, while the paper focused on a few schemes the techniques developed here are quite general and may play an important role in selecting and optimizing cluster methods for specific applications.

Acknowledgments

We thank A. Lichtenstein, A. Georges, S. Florens, S. Biermann for useful discussions, and M. Jarrell for pointing to us Ref. [16]. This work was supported by NSF grant N° DMR -0096462. We acknowledge the warm hospitality of the KITP program on Realistic Studies of Correlated Electrons, at UCSB (NSF grant PHY 99-07949) where part of this work was carried out, and the participants of this workshop for discussions.

APPENDIX A: REAL SPACE FORMULATION OF *DCA*

In this appendix, we present a real space formulation of *DCA* [8], which is useful for orders that break translation invariance. Let us consider first the translation invariant case. The hopping of the full lattice can be written using the reciprocal superlattice and the cluster indices (in real space) :

$$t_{\mu\nu}(K) = \frac{1}{L^d} \sum_{K_c} e^{i(K+K_c)\cdot(x_\mu-x_\nu)} t(K+K_c) \quad (\text{A1})$$

Here (in $d=1$), $-\frac{\pi}{L} \leq K \leq \frac{\pi}{L}$, $K_c = \frac{2\pi n}{L}$, $n = 0, \dots, L-1$ is on the reciprocal lattice of the (finite) cluster. Using $t_S = t$ in (7), we get *CDMFT*. Using $t_S = t^{cyc}$ with

$$t_{\mu\nu}^{cyc}(K) \equiv \frac{1}{L^d} \sum_{K_c} e^{iK_c\cdot(x_\mu-x_\nu)} t(K+K_c) \quad (\text{A2a})$$

$$= e^{-iKx_\mu} t_{\mu\nu}(K) e^{iKx_\nu} \quad (\text{A2b})$$

we get *DCA* . Indeed, t^{cyc} is cyclic in the cluster indices (by definition of K_c), and *provided that we obtain a translation invariant (cyclic) solution* we can diagonalize all matrices in the cluster to get Eq. (5).

Let us now consider the case where the solution of the real space formulation of *DCA* breaks the translation invariance in the cluster into a smaller invariance : the (big) cluster is divided into L_c^d small clusters of linear size L , and we have translation invariance in the big cluster when the small clusters are thought as collapsed into one point. For example, for AF order in $d = 1$, $L = 2$ (See Figure 3). We will then denote by $1 \leq \alpha, \beta \leq L$ the points in the small cluster, by $1 \leq A, B \leq L_c$ the positions of the small clusters in the big clusters, and by \bar{A}, \bar{B} the positions of the big clusters on the full lattice *expressed in units of the original lattice*. Any point on the big cluster can be described with a couple (α, A) and any point on the lattice by a triplet (α, A, \bar{A}) . Similarly, we denote by $-\pi \leq k \leq \pi$ an element of the original lattice’s Brillouin zone, by $-\pi/L \leq K \leq \pi/L$ an element of the Brillouin Zone of the superlattice of the small clusters, and by $-\pi/(LL_c) \leq \bar{K} \leq \pi/(LL_c)$ an element of the Brillouin Zone of the superlattice of the big

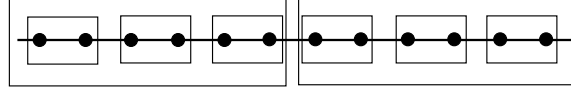


FIG. 3: Definition of big and small cluster in $d = 1$. $L = 2$, $L_c = 3$.

clusters. Finally, the reciprocal lattice of the small cluster are $K_c = \frac{2\pi n}{L}$, $n = 0, \dots, L-1$, the same for the big cluster considered as a cluster of L_c small clusters, in units of the original lattice, are $\bar{K}_c = \frac{1}{L} \frac{2\pi p}{L_c}$, $p = 0, \dots, L_c - 1$. Hence the reciprocal lattice points of the big cluster considered as a cluster of LL_c points are $\bar{K} + \bar{K}_c$. We solve the *DCA* in real space with the big cluster of size LL_c :

$$G_{\alpha A, \beta B}(\omega) = \sum_{\bar{K}} \frac{1}{\omega - t_{(\alpha, A), (\beta, B)}^{cyc}(\bar{K}) - \Sigma_{\alpha A, \beta B}(\omega)} \quad (\text{A3})$$

$$t_{(\alpha, A), (\beta, B)}^{cyc}(\bar{K}) = \frac{1}{(LL_c)^d} \sum_{K_c, \bar{K}_c} e^{i(K_c + \bar{K}_c) \cdot (x_\alpha + x_A - x_\beta - x_B)} t(\bar{K} + K_c + \bar{K}_c) \quad (\text{A4})$$

$$= \frac{1}{L_c^d} \sum_{\bar{K}_c} e^{i\bar{K}_c \cdot (x_\alpha + x_A - x_\beta - x_B)} t_{\alpha\beta}^{cyc}(\bar{K} + \bar{K}_c) \quad (\text{A5})$$

where we used $K_c \cdot x_A = 0$ [2π] in the last equation. Because of the reduced invariance, we can diagonalise using \bar{K}_c and obtain :

$$G_{\alpha\beta}(\bar{K}_c, \omega) = \sum_{\bar{K}} \frac{1}{\omega - t_{\alpha,\beta}^{cyc}(\bar{K} + \bar{K}_c) e^{i\bar{K}_c \cdot (x_\alpha - x_\beta)} - \Sigma_{\alpha,\beta}(\bar{K}_c, \omega)}$$

Using the *unitary* transformation :

$$\tilde{G}_{\alpha\beta}(\bar{K}_c, \omega) \equiv e^{-i\bar{K}_c \cdot (x_\alpha - x_\beta)} G_{\alpha\beta}(\bar{K}_c, \omega)$$

we obtain :

$$\tilde{G}_{\alpha\beta}(\bar{K}_c, \omega) = \sum_{\bar{K}} \frac{1}{\omega - t_{\alpha,\beta}^{cyc}(\bar{K} + \bar{K}_c) - \tilde{\Sigma}_{\alpha,\beta}(\bar{K}_c, \omega)} \quad (\text{A6})$$

Let us now concentrate on the AF order : $L = 2$ and for simplicity in dimension 1. In this case, $K_c = 0, \pi$. We will now show that (A6) is equivalent to the k -space formulation presented in [16] (denoted by a superscript M). In the AF phase, correlations appears between k and $k + \pi$ and the self-consistency condition reads :

$$G^M(\bar{K}_c, \omega) = \sum_{\bar{K}} \left(\begin{pmatrix} \omega - t(\bar{K} + \bar{K}_c) & 0 \\ 0 & \omega - t(\bar{K} + \bar{K}_c + \pi) \end{pmatrix} - \Sigma^M(\bar{K}_c, \omega) \right)^{-1} \quad (\text{A7})$$

where G^M and Σ^M are 2×2 matrices, which are non diagonal in the AF phase :

$$G^M \equiv - \begin{pmatrix} \langle T c_k c_k^\dagger \rangle & \langle T c_k c_{k+\pi}^\dagger \rangle \\ \langle T c_{k+\pi} c_k^\dagger \rangle & \langle T c_{k+\pi} c_{k+\pi}^\dagger \rangle \end{pmatrix}$$

Using the transformation [16]

$$c_{1K} = \frac{c_K + c_{K+\pi}}{\sqrt{2}} \quad c_{2K} = \frac{c_K - c_{K+\pi}}{\sqrt{2}}$$

Eq. (A7) is equivalent to (A6). Therefore the two formulations of *DCA* are equivalent in the antiferromagnetic phase.

The real space formulation of *DCA* share with *CDMFT* a property which is useful in practice : one doesn't have to *anticipate* the appearance of ordered phase, i.e. to adapt the cluster scheme for the order to be described. The order will show up automatically solving the real space *DCA* equations. Moreover, it can be more complex than an AF order, as long as the cluster is big enough to contain at least one unit cell.

APPENDIX B: LARGE- U LIMIT OF THE EFFECTIVE ACTION : PROOF OF (36)

Here, we present some details of the derivation of the large- U limit of Eq. (26), in the limit where $U \rightarrow \infty$ with $\beta \rightarrow \infty$, β/U fixed. The effective action is

$$S_{\text{eff}} = - \iint_0^\beta d\tau d\tau' c_{\mu\uparrow}^\dagger(\tau) G_{0,\mu\nu\uparrow}^{-1}(\tau, \tau') c_{\nu\uparrow}(\tau') + \int_0^\beta d\tau c_{\mu\downarrow}^\dagger(\tau) \partial_\tau c_{\mu\downarrow}(\tau) + U \left(n_{\mu\uparrow}(\tau) - \frac{1}{2} \right) \left(n_{\mu\downarrow}(\tau) - \frac{1}{2} \right) \quad (\text{B1})$$

$$G_{0,\mu\nu\uparrow}^{-1}(i\omega_n) = i \frac{xU}{2} \delta_{\mu\nu} - \tilde{t}_{\mu\nu}(x) - \frac{2t}{U} J_\rho^{\mu\nu}(x) \langle h_\rho \rangle + O\left(\frac{1}{U^2}\right) \quad (\text{B2})$$

We are going to compute the expression of partial partition function $Z[\{n_{\rho\downarrow}\}]$ (also denoted as $Z[\{S_\rho\}]$) as a function of the spins and and recover (36). We first compute the expansion of $\ln Z[\{n_{\rho\downarrow}\}]$ at second order in t and first order in J . We obtain :

$$\begin{aligned} \ln\left(\frac{Z[\{S_\rho\}]}{Z_0[\{S_\rho\}]}\right) &= \sum_{(i,j)} \sum_{i\omega_n, i\omega'_n} \tilde{t}_{ij}(i\omega_n) \tilde{t}_{ji}(i\omega'_n) \left\langle c_{i\uparrow}^\dagger(i\omega_n) c_{j\uparrow}(i\omega_n) c_{j\uparrow}^\dagger(i\omega'_n) c_{i\uparrow}(i\omega'_n) \right\rangle_S + \\ & 2 \sum_i \sum_{i\omega_n} J_\rho^{ii}(x) \langle h_\rho \rangle \left\langle c_{i\uparrow}^\dagger(i\omega_n) c_{i\uparrow}(i\omega_n) \right\rangle_S + O(t^3, J^2) \end{aligned} \quad (\text{B3})$$

where (i, j) denotes the sum over couples, $\langle \cdot \rangle_S$ is an average of the Gaussian action at fixed S . We see that

$$Z_0[\{S_\rho\}] \equiv Z_{t=J=0}[\{S_\rho\}] \propto \prod_\rho \cosh\left(\frac{\beta U}{4} S_\rho\right) \quad (\text{B4})$$

is independent of S_ρ (since $S_\rho = \pm 1$) and therefore it will be dropped in the following. Using the relations :

$$\left\langle c_\rho(i\omega_n) c_{\rho'}^\dagger(i\omega'_n) \right\rangle = -G_{\rho\rho'}^S(i\omega_n) \delta_{\omega_n, \omega'_n} \quad (\text{B5a})$$

$$G_{\rho\rho'}^S(i\omega_n) \equiv \frac{\delta_{\rho\rho'}}{i\omega_n + \frac{U}{2} S_\rho} = \frac{\delta_{\rho\rho'}}{2} \left(\frac{1 - S_\rho}{i\omega_n - \frac{U}{2}} + \frac{1 + S_\rho}{i\omega_n + \frac{U}{2}} \right) \quad (\text{B5b})$$

and the fact that in the AF phase $\tilde{t}(-z) = \tilde{t}(z)$ since $\langle S_i \rangle + \langle S_j \rangle = 0$, we can reduce the expression (B3), extract the $S_i S_j$ term and obtain finally :

$$\ln(Z[\{S_\rho\}]) = -\beta H_{\text{eff}} + O(t^3, J^2) \quad (\text{B6})$$

with H_{eff} given by Eqs. (36). The additional term $J_\rho^{\mu\nu}$ does not contribute to the J_{Ising} since it would give a $O(1/U^2)$ contribution. Moreover, since $J_{\text{Ising}} \sim \tilde{t}^2/U$ we do not need to compute the $1/U$ term of Σ^C .

Finally, higher orders in the expansion do not contribute. Indeed, since $Z[\{S_\rho\}]$ is a *gaussian* action and since we compute $\ln Z[\{S_\rho\}]/Z_0$, we only get *connected diagrams*, thus we have one sum over Matsubara frequencies. Each Matsubara sum gives a factor βU (in the large- U limit \sum_{ω_n} is replaced by $\frac{\beta}{4\pi} \int d(xU)$) and each G a factor U^{-1} . Therefore higher order terms are subdominant.

APPENDIX C: CLASSICAL LIMIT OF PCDMFT

In this Appendix, we present the solution of Eqs. (9,29,33) for completeness. We restrict ourselves to nearest neighbor hopping. We start by solving at order 1 in the $1/U$ expansion. From (29) and (33), we have for $\mu \neq \nu$ ($\Delta_{\mu\mu} = 0$):

$$\Delta_{\mu\nu}^\alpha = t_{\nu-\mu} + \overline{\delta\Sigma_{\mu\nu}^{\text{latt}^\alpha}} - \Delta_{\mu\nu}^\alpha \frac{\langle h_\mu^\alpha h_\nu^\alpha \rangle_c}{\langle h_\mu^\alpha \rangle \langle h_\nu^\alpha \rangle} \quad (\text{C1})$$

where $\alpha = 1, 2$ is an index for the two (AF) solutions as in (9). Dividing the cluster into its two sublattices A and B with $\mathcal{C} = \mathcal{C}_A \cup \mathcal{C}_B$ and using (9), we have (for all $\mu \in \mathcal{C}$) :

$$\overline{\delta\Sigma_{\mu, \mu+\delta}^{\text{latt}^\alpha}} = \frac{1}{S_c} \sum_{\substack{\rho \in \mathcal{C}_A \\ \rho+\delta \in \mathcal{C}}} \delta\Sigma_{\rho, \rho+\delta}^{C^\beta} + \frac{1}{S_c} \sum_{\substack{\rho \in \mathcal{C}_B \\ \rho+\delta \in \mathcal{C}}} \delta\Sigma_{\rho, \rho+\delta}^{C^\beta} \quad (\text{C2})$$

where $\beta = \alpha$ if $\mu \in \mathcal{C}_A$, $\beta = \bar{\alpha}$ otherwise, since if $\rho + \delta \notin \mathcal{C}$, the exponential depends on K and averages to zero. For $\mu, \mu + \delta \in \mathcal{C}$, Eq. (C1) leads to :

$$\Delta_{\mu, \mu+\delta}^{\alpha} \frac{\langle h_{\mu}^{\alpha} h_{\mu+\delta}^{\alpha} \rangle}{\langle h_{\mu}^{\alpha} \rangle \langle h_{\mu+\delta}^{\alpha} \rangle} = t_{\delta} + \frac{1}{S_c} \sum_{\substack{\rho \in \mathcal{C}_A \\ \rho+\delta \in \mathcal{C}}} \Delta_{\rho, \rho+\delta}^{\beta} \frac{\langle h_{\rho}^{\beta} h_{\rho+\delta}^{\beta} \rangle_c}{\langle h_{\rho}^{\beta} \rangle \langle h_{\rho+\delta}^{\beta} \rangle} + \frac{1}{S_c} \sum_{\substack{\rho \in \mathcal{C}_B \\ \rho+\delta \in \mathcal{C}}} \Delta_{\rho, \rho+\delta}^{\bar{\beta}} \frac{\langle h_{\rho}^{\bar{\beta}} h_{\rho+\delta}^{\bar{\beta}} \rangle_c}{\langle h_{\rho}^{\bar{\beta}} \rangle \langle h_{\rho+\delta}^{\bar{\beta}} \rangle} \quad (\text{C3})$$

for all μ, δ . The left hand side depends only on whether $\mu \in \mathcal{C}_A$ or not. Therefore, for all δ , we can define for $\mu \in \mathcal{C}_A$ and $\zeta \in \mathcal{C}_B$:

$$F_{\delta}^{\alpha A} \equiv \Delta_{\mu, \mu+\delta}^{\alpha} \frac{\langle h_{\mu}^{\alpha} h_{\mu+\delta}^{\alpha} \rangle}{\langle h_{\mu}^{\alpha} \rangle \langle h_{\mu+\delta}^{\alpha} \rangle} \quad (\text{C4a})$$

$$F_{\delta}^{\alpha B} \equiv \Delta_{\zeta, \zeta+\delta}^{\alpha} \frac{\langle h_{\zeta}^{\alpha} h_{\zeta+\delta}^{\alpha} \rangle}{\langle h_{\zeta}^{\alpha} \rangle \langle h_{\zeta+\delta}^{\alpha} \rangle} \quad (\text{C4b})$$

(they are independent of μ and ζ). Eq. (C3) then leads to :

$$F_{\delta}^{\alpha A} = t_{\delta} + A_{\delta\alpha} F_{\delta}^{\alpha A} + B_{\delta\alpha} F_{\delta}^{\bar{\alpha} B} \quad (\text{C5a})$$

$$F_{\delta}^{\alpha B} = t_{\delta} + A_{\delta\bar{\alpha}} F_{\delta}^{\bar{\alpha} A} + B_{\delta\bar{\alpha}} F_{\delta}^{\alpha B} \quad (\text{C5b})$$

$$A_{\delta\alpha} \equiv \frac{1}{S_c} \sum_{\substack{\rho \in \mathcal{C}_A \\ \rho+\delta \in \mathcal{C}}} \frac{\langle h_{\rho}^{\alpha} h_{\rho+\delta}^{\alpha} \rangle_c}{\langle h_{\rho}^{\alpha} \rangle \langle h_{\rho+\delta}^{\alpha} \rangle} \quad B_{\delta\alpha} \equiv \frac{1}{S_c} \sum_{\substack{\rho \in \mathcal{C}_B \\ \rho+\delta \in \mathcal{C}}} \frac{\langle h_{\rho}^{\bar{\alpha}} h_{\rho+\delta}^{\bar{\alpha}} \rangle_c}{\langle h_{\rho}^{\bar{\alpha}} \rangle \langle h_{\rho+\delta}^{\bar{\alpha}} \rangle} \quad (\text{C5c})$$

which can be rewritten as :

$$(1 - A_{\delta\alpha}) F_{\delta}^{\alpha A} - B_{\delta\alpha} F_{\delta}^{\bar{\alpha} B} = t_{\delta} \quad (\text{C6a})$$

$$(1 - B_{\delta\alpha}) F_{\delta}^{\bar{\alpha} B} - A_{\delta\alpha} F_{\delta}^{\alpha A} = t_{\delta} \quad (\text{C6b})$$

The determinant of the equations for F is given by $\prod_{\alpha} (1 - A_{\delta\alpha} - B_{\delta\alpha})$, which does not vanish for a generic x . For $|\delta| > 1$, $t_{\delta} = 0$ by assumption hence $F_{\delta}^{\alpha A/B} = 0$. In the classical limit, the two solutions are related by a spin-flip, so $\frac{\langle h_{\nu}^{\alpha} h_{\nu}^{\alpha} \rangle_c}{\langle h_{\nu}^{\alpha} \rangle \langle h_{\nu}^{\alpha} \rangle}$ does not depend on α for μ, ν nearest neighbor, according to (31). For $|\delta| = 1$, the unique solution is obtained for equal $F_{\delta} \equiv F_{\delta}^{\alpha A/B}$, which is given by :

$$F_{\delta} = \frac{t_{\delta}}{1 - \frac{1}{S_c} \sum_{\substack{\rho \in \mathcal{C} \\ \rho+\delta \in \mathcal{C}}} \frac{\langle h_{\rho} h_{\rho+\delta} \rangle_c}{\langle h_{\rho} \rangle \langle h_{\rho+\delta} \rangle}} \quad (\text{C7})$$

Using the square symmetry, one can pick up one δ to compute the denominator. Hence, we obtain Eq. (40a) and (40c) (the hopping is nearest neighbors). Note that the hopping is renormalised at order 1 (in $1/U$), but it is still restricted to nearest neighbors. In order to compute the J term, we now focus on $t + \delta \Sigma^{\text{latt}}$ which satisfies :

$$\overline{(t + \delta \Sigma^{\text{latt}})}_{\mu, \mu+\delta} = F_{\delta} \quad (\text{C8})$$

It is a translation invariant quantity, which is also restricted to nearest neighbors. It has a formula analogous to (A1) for the hopping, and its value inside the cluster is given by its K average. Using (33c) to compute the mean field terms $J_{\nu}^{\mu\mu}$, we see that the computation is similar than for $CDMFT$, with just a renormalisation of the hopping (note however that $t + \delta \Sigma^{\text{latt}}$ is *not* the effective hopping \tilde{t} defined as the order 1 term of Δ). In particular, the J_B terms have the same range as the original lattice hopping. Reporting (C8) into (33c) leads to Eq. (40a), which completes the derivation.

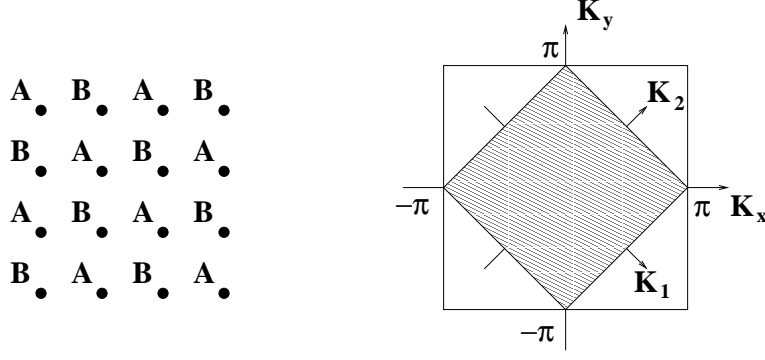


FIG. 4: Notations and reduced Brillouin zone for the pair scheme (shaded area)

APPENDIX D: CLASSICAL LIMIT OF THE PAIR SCHEME

The first task is to generalise the pair scheme in the presence of antiferromagnetic order. Denoting the two sublattices by A and B , we have the approximation for Φ :

$$\Phi_{pair} = (1 - z) \left(\sum_{i \in A} \Phi_1[G_{ii}] + \sum_{j \in B} \Phi_1[G_{jj}] \right) + \sum_{\substack{\langle ij \rangle \\ i \in A \\ j \in B}} \Phi_2[G_{ii}, G_{jj}, G_{ij}] \quad (\text{D1})$$

We denote by (1) and (2) the one site and the two site model respectively. We group the two one-site models into 2×2 diagonal matrices, and denote with an index *diag* the diagonal part of a matrix. To write the self-consistency condition, we take as unit cell one site on A , one site on B . K is now a vector in the corresponding reduced Brillouin zone, presented on Figure 4. The hopping and the lattice self-energy are given by :

$$t_{AA}(K) = t_{BB}(K) = 0 \quad (\text{D2a})$$

$$t_{AB}(K) = tC(K) \quad (\text{D2b})$$

$$C(K) = 1 + e^{-i(K_1 - K_2)} + e^{i(K_1 - K_2)} + e^{-i(K_1 + K_2)} \quad (\text{D2c})$$

$$\Sigma_{diag}^{latt}(K) = \Sigma^{loc} = (1 - z)\Sigma_{diag}^{(1)} + z\Sigma_{diag}^{(2)} \quad (\text{D2d})$$

$$\Sigma_{AB}^{latt}(K) = \Sigma_{12}^{(2)} C(K) \quad (\text{D2e})$$

and the Green function by the usual formula (with 2×2 matrices).

$$G = \overline{(i\omega_n - t(K) - \Sigma^{latt}(K, i\omega_n))^{-1}}$$

The scheme implies a consistency equations for the Green functions :

$$G^{(2)} = G$$

$$G^{(1)} = D(G)$$

where we denote by D the linear operator that restricts a matrix to its diagonal.

First $G_{0\downarrow}$ is diagonal (with same proof as for the other schemes) but here it is not trivial :

$$(G_{0\downarrow}^{(1)})^{-1}(i\omega_n) = i\omega_n + \Sigma_{\downarrow}^{(1)}(i\omega_n) - \Sigma_{\downarrow}^{latt}(i\omega_n) = i\omega_n - z \left(\Sigma_{\downarrow}^{(2)}(i\omega_n) - \Sigma_{\downarrow}^{(1)}(i\omega_n) \right) \quad (\text{D3})$$

$$(G_{0\downarrow}^{(2)})^{-1}(i\omega_n) = i\omega_n + \Sigma_{\downarrow}^{(2)}(i\omega_n) - \Sigma_{\downarrow}^{latt}(i\omega_n) = i\omega_n - (z - 1) \left(\Sigma_{\downarrow}^{(2)}(i\omega_n) - \Sigma_{\downarrow}^{(1)}(i\omega_n) \right) \quad (\text{D4})$$

Using previous notations, we have :

$$\frac{\Delta_{\downarrow}^{(1)}(x)}{\Delta_{\downarrow}^{(2)}(x)} = \frac{z}{z - 1} \quad (\text{D5})$$

Let's turn now to the up electrons. Introducing the notations :

$$\begin{aligned}\bar{A}^{(2)} &= \bar{A} \\ \bar{A}^{(1)} &= \overline{D(\bar{A})}\end{aligned}$$

and, using that, for d a diagonal matrix independant of K , $\overline{Ad}^{(\alpha)} = \bar{A}^{(\alpha)}d$ (for $\alpha = 1, 2$), we can expand the self-consistency conditions :

$$\left(G_0^{(1)}\right)^{-1} = \left(G^{(1)}\right)^{-1} + \Sigma^{(1)} \quad (\text{D6})$$

$$\left(G_0^{(2)}\right)^{-1} = \left(G^{(2)}\right)^{-1} + \Sigma^{(2)} \quad (\text{D7})$$

with the expansion (33), to get :

$$\Delta_{ii}^{(\alpha)}(x) = \overline{t_{ii}}^{(\alpha)} + \Sigma_{ii}^{loc} - \Sigma_{ii}^{(\alpha)} + \frac{2t}{U} J_{ii\rho}^{(\alpha)}(x) \langle h_\rho^{(\alpha)} \rangle + O\left(\frac{1}{U^2}\right) \quad (\alpha, i = 1, 2) \quad (\text{D8a})$$

$$J_{\mu\nu\rho}^{(\alpha)}(x) \equiv \frac{1}{t} \left(\overline{t_{\mu\rho} t_{\rho\nu}}^{(\alpha)} - \overline{t_{\mu\rho}}^{(\alpha)} \overline{t_{\rho\nu}}^{(\alpha)} \right) \quad (\text{D8b})$$

$$\tilde{t}(K, x) \equiv t(K) + \Sigma^{\text{latt}}(K, x) \quad (\text{D8c})$$

Clearly, $\rho = \bar{i}$ with the notation $\bar{2} = 1, \bar{1} = 2$. Moreover,

$$\overline{\Sigma}_{diag}^{\text{latt}(1)} - \Sigma^{(1)} = z \left(\Sigma_{diag}^{(2)} - \Sigma^{(1)} \right) \quad (\text{D9a})$$

$$\overline{\Sigma}_{diag}^{\text{latt}(2)} - \Sigma^{(2)} = (z - 1) \left(\Sigma_{diag}^{(2)} - \Sigma^{(1)} \right) \quad (\text{D9b})$$

and the J terms are given by :

$$J^{(1)} = \frac{1}{t} \sum_R \tilde{t}_{\mu\rho}(R) \tilde{t}_{\rho\nu}(-R) \quad (\text{D10a})$$

$$J^{(2)} = \frac{1}{t} \sum_{R \neq 0} \tilde{t}_{\mu\rho}(R) \tilde{t}_{\rho\nu}(-R) \quad (\text{D10b})$$

which implies

$$J^{(1)} = z J_0 \quad (\text{D11a})$$

$$J^{(2)} = (z - 1) J_0 \quad (\text{D11b})$$

Therefore the equations for Δ simplify into :

$$\Delta_{\uparrow ii}^{(1)} = z \left(\Sigma_{diag}^{(2)} - \Sigma^{(1)} \right) + 2z J_0 \langle h_i^{(1)} \rangle \quad (\text{D12a})$$

$$\Delta_{\uparrow ii}^{(2)} = (z - 1) \left(\Sigma_{diag}^{(2)} - \Sigma^{(1)} \right) + 2(z - 1) J_0 \langle h_i^{(2)} \rangle \quad (\text{D12b})$$

Using that $m^{(1)} = m^{(2)}$, we have $\langle h_i^{(2)} \rangle = \langle h_i^{(1)} \rangle$ at dominant order and therefore

$$\frac{\Delta_{\uparrow ii}^{(2)}}{\Delta_{\uparrow ii}^{(1)}} = \frac{z - 1}{z} \quad (\text{D13})$$

From (D5,D13), using the computation of the classical field from Δ presented in Appendix B, we obtain the *classical variation method* defined in (41,42).

Strictly speaking, we only prove here that, in the large- U limit, if there is a magnetic solution, it obeys the CVM equations. We have not shown that such non zero solution exist. A priori, one could wish to push the semi-classical computation further and *compute* the classical field explicitly to check that it gives the values prescribed by the consistency of the classical equations. However, this is much harder to do than in previous schemes for the following reason : contrary to all other schemes studied in this paper, there is no cancellation between the diagonal part of Σ^{latt} and of Σ^{C} . Therefore, we have to compute correction to $\langle h \rangle$ to order $1/U^2$, in order to compute Δ to order $1/U$ (the relation (30a) is a priori valid only at dominant order). Because $\beta \sim U$, we need Δ up to order $1/U^3$ to get the such correction (like we need Δ at order $1/U$ to get a classical field of order 1). All these difficulties are hidden in the $\Sigma_{diag}^{(2)} - \Sigma^{(1)}$ term in (D12).

APPENDIX E: PROOF OF THE CUTKOVSKY-T'HOOF-T-VELTMAN EQUATION

In this appendix, we prove the Cutkovsky-t'Hooft-Veltman formula using the Keldysh method [24]. We first briefly present our conventions.

1. Notations

We denote with a + the upper contour (going from $-\infty$ to ∞) and a - the lower contour. The definition of the Keldysh propagators (for fermions) is:

$$-i \langle T\phi(x,t)\phi^\dagger(x',t') \rangle = G^{++}(x, x', t - t') \quad (\text{E1})$$

$$-i \langle \tilde{T}\phi(x,t)\phi^\dagger(x',t') \rangle = G^{--}(x, x', t - t') \quad (\text{E2})$$

$$i \langle \phi^\dagger(x',t')\phi(x,t) \rangle = G^{+-}(x, x', t - t') \quad (\text{E3})$$

$$-i \langle \phi(x,t)\phi^\dagger(x',t') \rangle = G^{-+}(x, x', t - t') \quad (\text{E4})$$

After Fourier transformation ($\hat{f}(\omega) = \int dt e^{i\omega t} f(t)$), we have in particular the following useful relations :

$$\rho(x, x', \omega) = -\frac{1}{\pi} \text{Im} G_R(x, x', \omega) \quad (\text{E5a})$$

$$G^{+-}(x, x', \omega) = 2i\pi\rho(x, x', \omega)\theta(-\omega) \quad (\text{E5b})$$

$$G^{-+}(x, x', \omega) = -2i\pi\rho(x, x', \omega)\theta(\omega) \quad (\text{E5c})$$

$$(G^{++}(x, x', \omega))^* = -G^{--}(x', x, \omega) \quad (\text{E5d})$$

To illustrate the diagrammatics, consider for example as an example a second order self-energy diagram in Fig. 5. It

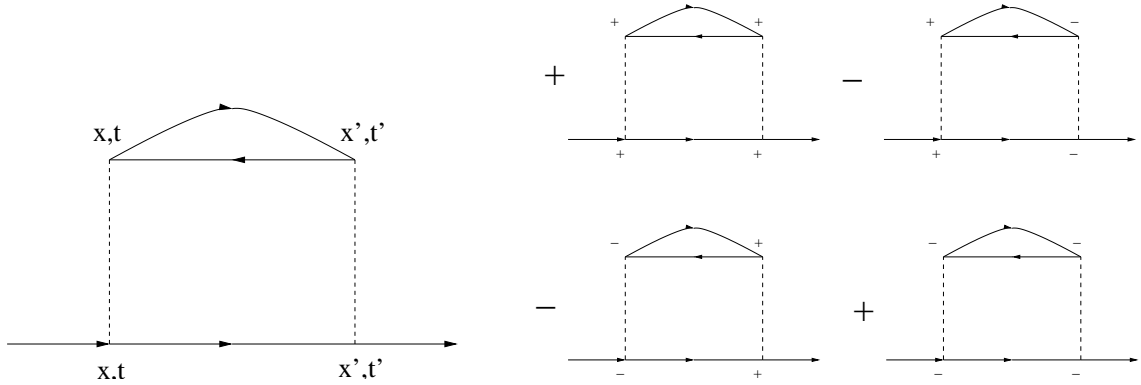


FIG. 5: A self energy diagram and its Keldysh counterparts, with the Keldysh indices and the overall factor.

corresponds to

$$G_{x,x',t-t'} G_{x,x',t-t'} G_{x',x,t'-t}$$

The Keldysh counterparts of the diagram are obtained by replacing each vertex by his corresponding Keldysh counterpart (See Fig 5). They corresponds to:

$$G_{x,x',t-t'}^{++} G_{x,x',t-t'}^{++} G_{x',x,t'-t}^{++} - G_{x,x',t-t'}^{+-} G_{x,x',t-t'}^{+-} G_{x',x,t'-t}^{+-} - G_{x,x',t-t'}^{-+} G_{x,x',t-t'}^{-+} G_{x',x,t'-t}^{-+} + G_{x,x',t-t'}^{--} G_{x,x',t-t'}^{--} G_{x',x,t'-t}^{--}$$

where $G^{\pm,\pm}$ are the Keldysh propagators.

2. Proof

The first point is to write the imaginary part of the zero-temperature retarded self energy in terms of the Keldysh components :

$$\text{Im}\Sigma_R(\omega) = \frac{\Sigma_{+-}(\omega) - \Sigma_{-+}(\omega)}{2i} \quad (\text{E6})$$

An important point is that this relation must hold *for each diagram individually*, in order to be compatible with any approximation considered as a diagram summation. Indeed at $T = 0$ for $\omega > 0$

$$\Sigma_R(\omega) = \frac{1}{2i}(\Sigma_{++}(\omega) + \Sigma_{+-}(\omega))$$

and using (E5b,E5c), it is sufficient to prove that

$$\Sigma^{++} + \Sigma^{--} + \Sigma^{+-} + \Sigma^{-+} = 0 \quad (\text{E7})$$

is verified *for each diagram individually*. A way to prove that, which is actually in Veltman's book[21], consists in noticing that each diagram with a $+$ at the largest time vertex cancels against the same diagram with a $-$ at this largest time vertex. This happens because $G^{++}(t-t') = G^{-+}(t-t')$ and $G^{--}(t-t') = G^{+-}(t-t')$ for $t > t'$ so the only thing that changes between one diagram and the other is a minus sign (associated with the $-$ vertex and not to the $+$ vertex). This is called by Veltman *the largest time equation*. To unveil this relationship we use the following notation: circle a vertex if it corresponds to ϕ^- and do not circle it if it corresponds to ϕ^+ . Then the relationship with Veltman rules to obtain the largest time equation will become clear.

To obtain the Keldysh expansion of $\text{Im}\Sigma_R$, we can thus take the expansion of Σ (as defined with any perturbation theory) and put Keldysh indices on it (as explained in paragraph E1). First, we will focus on $\omega > 0$. Then $\Sigma_{+-}(\omega) = 0$, we only need to compute Σ_{-+} , *i.e.* the diagram with a $+$ at the incoming vertex, and a $-$ at the outgoing vertex. The crucial properties of **zero-temperature** diagrams is the following : due to the presence of θ functions in frequency for G^{+-} and G^{-+} (Cf. paragraph E1), the frequency flows always from the $+$ vertex to the $-$ vertex. This implies that a diagram is zero if it contains a $-$ vertex to which no external line is connected and that is surrounded by $+$ vertices because of frequency conservation (the same is true if one replace $+$ with $-$). This cancellation generalizes to a connected set, or region, of $-$ to which no external line is connected and that is surrounded by $+$ vertices. Since we only have two external vertices, the non-vanishing diagrams are those with a line that cut propagators dividing them into a $+$ region L on the left (connected to the incoming vertex) and a $-$ region R on the right (connected to the outgoing vertex). This line is the cut of the diagram and the sum over Keldysh indices reduces to the sum over all possible cuts. (see Fig. 1). In the L (resp. R) region, we have to use G^{++} (resp. G^{--}). Since $G^{--}(x, x', \omega) = -(G^{++}(x', x, \omega))^*$, the R part gives D_{MR}^* times $(-1)^{\text{number of internal lines}}$, where MR is the (left) diagram part obtained from R by inverting all the arrows. Finally, to each cut line going from right to left (left to right) is associated a G^{+-} (G^{-+}) propagator. Hence we obtain the third rule of the text : each cut lines going from left to right (right to left) is replaced by $\rho(x, x', \omega)\theta(\omega)$ ($\rho(x, x', \omega)\theta(-\omega)$).

So there are two last things that remains to be clarified in order to get the eq. (44): (1) that the symmetry factors are taking into account correctly and (2) that the phase between the half left and right diagram is the one leading to eq. (44). Concerning the symmetry factors one has to be sure that all the counting is done correctly. In order to do this is useful to replace each half (or left) diagram with the sum of all half diagrams obtained from the original one permuting the cut lines in all the possible ways. The symmetry factor that one has to attach to them is exactly the one needed to get back the right symmetry factor for the original diagram by gluing together the half-right and the half-left diagrams. The "gluing" operations means attach to each i line (see fig. 2) of the half diagram the corresponding i line of the left diagrams. Indeed to get the symmetry factor of a given diagram one has to write all the topologically equivalent way to obtain the same diagram. This can be done starting from the left and from the right, *i.e.* writing all the different ways to get the same topologically equivalent left and right diagrams and then attach them in all the possible ways that give rise to the original diagram. Thus, the symmetry factor related to a half or left diagrams are just all the different ways (contractions) that can be used to create them. In this way the operation of "gluing" together a half and left diagram in which all the cut lines have been permuted produces $n!$ (n is the number of cut lines) times the original uncut diagrams. The $1/n!$ in eq. 47 is there exactly to balance this redundant $n!$ term.

Finally, let us focus on the phase between the right part of the diagram and D_{MR}^* is

$$a = (-1)^{l_R} (-1)^{v_{\alpha R}} (-1)^{v_{\alpha R}(n_{\alpha}+1)} (-1)^{n_{loop}} (-i)^n (i)^{n-1} \quad (\text{E8})$$

The first term comes from the sign in $G^{--} = -G^{++*}$, with l_R the number of internal lines inside the right part R ; the second comes from the $-$ Keldysh vertices, with $v_{\alpha R}$ the number of vertices of type α in the right part; the third comes from the $(-i)^{n_{\alpha}+1}$ factor of each vertices at $T = 0$ with n_{α} the number of outgoing lines in the vertices of type α : this factor change under conjugation; the fourth comes from the n_{loop} broken loops in the cut diagrams (we restrict ourselves for fermions here); the fifth and sixth terms comes from the difference between G_{+-} and ρ (in the cut propagators going from left to right and right to left respectively). The number of cut loops is given by $n_{loop} = n - 1$. Moreover, summing all lines ending at a vertex in the right part, we have :

$$\sum_{\alpha} v_{\alpha R} n_{\alpha} = l_R + n \quad [2] \quad (E9)$$

where [2] is the reduction modulo 2. Finally we get $a = i$ which, combined with (E6) leads to the Eq. (44). Similarly, for $\omega < 0$, we have $\text{Im}\Sigma_R = \Sigma_{+-}/2i$. The left part has $-$ vertices, the right part $+$ vertices. Using a similar analysis, we get $a = -i$, which leads to Eq. (44).

-
- [1] A. Georges, G. Kotliar, W. Krauth and M.J. Rozenberg, Rev. Mod. Phys. **68** 13 (1996).
[2] S. Savrasov, G. Kotliar and E. Abrahams, Nature **410** 793 (2001); S. Biermann, F. Aryasetiawan and A. Georges, Phys. Rev. Lett **90** 086402 (2003).
[3] V. Dobrosavljevic and G. Kotliar, Phys. Rev. B **50** 1430 (1994); V. Dobrosavljevic and G. Kotliar, Acta Polonica **85** 21 (1994).
[4] Q. Si and J.L. Smith, Phys. Rev. Lett **77** 3391 (1996); J.L. Smith and Q. Si, Phys. Rev. B **61** 5184 (2000).
[5] A. Schiller and K. Ingersent, Phys. Rev. Lett **75** 113 (1995).
[6] G. Zarand, D. Cox and A. Schiller, Phys. Rev. B **62** R16227 (2000).
[7] T. Maier, M. Jarrell, T. Pruschke and J. Keller, Eur. Phys. J. B **13** 613 (2000); M.H. Hettler, A.N. Tahvildar-Zadeh, M. Jarrell, T. Pruschke and H.R. Krishnamurthy, Phys. Rev. B **58** R7475 (1998).
[8] G. Biroli and G. Kotliar, Phys. Rev. B **65** 155112 (2002).
[9] G. Kotliar, S.Y. Savrasov, G. Pálsson and G. Biroli, Phys. Rev. Lett **87** 186401 (2001).
[10] T.A. Maier and M. Jarrell, Phys. Rev. B **65** 041104 (2002).
[11] C.J. Bolech, S.S. Kancharla and G. Kotliar, Phys. Rev. B **67** 075110 (2003).
[12] A. Lichtenstein, Private Communication.
[13] A.I. Lichtenstein and M.I. Katsnelson, Phys. Rev. B **62** R9283 (2000).
[14] S. Pankov, G. Kotliar and Y. Motome, Phys. Rev. B **66** 045117 (2002).
[15] R. Mills and P. Ratanavararaksa, Phys. Rev. B **18** 5291 (1978); R. Mills, T. Kaplan, and L.J. Gray, Phys. Rev. B **27** 3252 (1983).
[16] T.A. Maier, http://www.physics.uc.edu/~jarrell/thesis_tmaier.ps.gz.
[17] R. Kikuchi, Phys. Rev. **81** 988 (1951).
[18] T. Morita, J. Stat. Phys. **59** 819 (1990).
[19] B.G. Nickel and W.H. Butler, Phys. Rev. Lett **30** 373 (1973).
[20] J.K. Freericks and V. Zlatic, cond-mat/0301188.
[21] "Diagrammatica" M. Veltman, *Cambridge Lecture Notes in Physics* (1994).
[22] S. Okamoto, A.J. Millis, H. Monien and A. Fuhrmann, cond-mat/0306178.
[23] M. Capone and M. Civelli, unpublished.
[24] L.V. Keldysh, Sov. Phys. JETP **20** 1018 (1965); J. Rammer and H. Smith, Rev. Mod. Phys. **58** 323 (1986).